

For Reference

NOT TO BE TAKEN FROM THIS ROOM

Ex libris
UNIVERSITATIS
ALBERTAENSIS





Digitized by the Internet Archive
in 2020 with funding from
University of Alberta Libraries

<https://archive.org/details/Olson1980>

THE UNIVERSITY OF ALBERTA

RELEASE FORM

NAME OF AUTHOR: Arthur Randall Olson

TITLE OF THESIS: In Vitro Placental Pollination and Seed Development
in Papaver nudicaule L.

DEGREE FOR WHICH THESIS WAS PRESENTED: Doctor of Philosophy

YEAR THIS DEGREE GRANTED: 1980

Permission is hereby granted to THE UNIVERSITY OF ALBERTA LIBRARY to reproduce single copies of this thesis and to lend or sell such copies for private, scholarly or scientific research purposes only.

The author reserves other publication rights, and neither the thesis nor extensive extracts from it may be printed or otherwise reproduced without the author's written permission.



THE UNIVERSITY OF ALBERTA

IN VITRO PLACENTAL POLLINATION AND SEED DEVELOPMENT

IN PAPAYER NUDICAULE L.

by



ARTHUR RANDALL OLSON

A THESIS

SUBMITTED TO THE FACULTY OF GRADUATE STUDIES AND RESEARCH

IN PARTIAL FULFILMENT OF THE REQUIREMENTS FOR THE DEGREE

OF DOCTOR OF PHILOSOPHY

IN

STRUCTURAL BOTANY

DEPARTMENT OF BOTANY

EDMONTON, ALBERTA

FALL 1980

THE UNIVERSITY OF ALBERTA
FACULTY OF GRADUATE STUDIES AND RESEARCH

The undersigned certify that they have read, and recommend to the Faculty of Graduate Studies and Research, for acceptance, a thesis entitled "In Vitro Placental Pollination and Seed Development in Papaver nudicaule L." submitted by Arthur Randall Olson in partial fulfilment of the requirements for the degree of Doctor of Philosophy in Structural Botany.



To Vicki, who shares in all I do.

ABSTRACT

Successful fertilization and seed development following placental pollination in vitro has been reported in several angiosperms. In Papaver nudicaule L., placentae with attached ovules were dissected out of unpollinated gynoecia 1-3 days after anthesis, dusted with pollen, and cultured on modified Nitsch's growth medium at 23C. For comparison, greenhouse flowers were hand-pollinated on the day of anthesis and allowed to continue development in vivo. Fertilized ovules at different stages were fixed in GA-OsO₄, embedded in Spurr's resin, and processed for light microscopic and certain histochemical techniques. Pollen germinates after one hour in vitro. Although most pollen tube growth appears random, there is directional growth toward the micropyle. The crassinucellate ovule contains a Polygonum-type megagametophyte. The polarized egg has a large chalazal vacuole and micropylar nucleus. Pollen tube access into the megagametophyte is through a degenerate synergid with fertilization occurring between 24 and 31 hours after pollination in vitro. Zygote establishment is accompanied by polarity reversal in which the nucleus assumes the chalazal position subtended by a large micropylar vacuole. Three days after pollination in vitro a two-celled proembryo and free nuclear endosperm are established. Endosperm cellularization occurs after 4-5 days in culture. At day 10 of incubation endosperm cytoplasm is dense and there is a large globular embryo. Substantial interdigitation between presumptive protodermal outer tangential walls and adjacent endosperm appears at this time. Protoderm crenulations are presumably related to aspects of endosperm degradation. The

primary meristems and their derivative tissues are discernable between 12 and 15 days when cotyledon initiation occurs. Embryos achieve morphological maturity within 27-28 days and most seeds are germinable. In vitro placental pollination and seed development techniques provide a useful experimental research tool and may also have economic implications.

ACKNOWLEDGMENTS

I am indebted to my supervisor, Dr. David D. Cass, for his generosity with both time and N.S.E.R.C. funds (grant A-6103) in supporting this study. Throughout my study under his direction, Dave Cass has been, above all, a good friend. The support and advice given by Dr. James M. Mayo, Dr. Ruth A. Stockey, and Scott D. Russell was greatly appreciated. Special thanks to Mr. Rudi Kroon, Mr. Hermann Barthel, and Ms. Lillian Barei of the University of Alberta Botany Greenhouses for their endeavours to keep me supplied with flowers. I also thank Jim Basinger who was both friend and sounding board. In addition to giving me strength through her loving support during this study, I wish to thank my dear wife, Vicki, who actually found the courage to face the task of typing this thesis.

TABLE OF CONTENTS

CHAPTER		PAGE
1.	INTRODUCTION.....	1
2.	POLLINATION.....	6
	Materials and Methods.....	6
	Pre-fertilization Ovule.....	7
	General morphology.....	7
	Integuments.....	8
	Nucellus.....	8
	Megagametophyte.....	10
	Synergids.....	10
	Egg.....	11
	Central cell.....	12
	Antipodals.....	14
	Pollination Events.....	15
	Pollen germination.....	15
	Path of the pollen tube.....	16
	Discussion.....	18
3.	SEED DEVELOPMENT.....	24
	Materials and Methods.....	24
	Post-fertilization Ovule <u>In Vitro</u>	25
	Embryogenesis.....	25
	Zygote.....	25

CHAPTER	PAGE
Proembryo.....	27
Early globular embryo.....	28
Late globular embryo.....	29
Cotyledon initiation.....	29
Epicotyl.....	31
Hypocotyl.....	32
Endosperm development.....	34
Endosperm degradation.....	36
Synergids.....	39
Antipodals.....	40
Nucellus.....	42
Seed coat.....	43
Inner integument.....	43
Outer integument.....	44
Development without placental attachment.....	45
Post-fertilization Ovule <u>In Vivo</u>	46
Early seed development.....	46
Mature seed structure.....	49
Discussion.....	50
4. SUMMARY AND CONCLUSIONS.....	91
BIBLIOGRAPHY.....	96
APPENDIX ONE.....	105
APPENDIX TWO.....	109

LIST OF FIGURES

FIGURE	PAGE
1. Scanning electron micrograph of pre-pollination ovule	62
2. Scanning electron micrograph of ventral surface of pre-pollination, detached ovule.....	62
3. Scanning electron micrograph of ovules 15 hrs. post-pollination <u>in vitro</u>	62
4. Scanning electron micrograph of germinated pollen grain 6 hrs. post-pollination <u>in vitro</u>	62
5. Light micrograph of longitudinal section through pre-fertilization synergids.....	64
6. Light micrograph of longitudinal section through egg.....	64
7. Light micrograph of longitudinal section through chalazal end of a pre-fertilization ovule.....	64
8. Light micrograph of secondary nucleus (SN) situated in chalazal region of central cell adjacent to antipodals.....	64
9. Scanning electron micrograph of ovule penetrated by pollen tube 15 hrs. post-pollination <u>in vitro</u>	66
10. Light micrograph of longitudinal section through pre-fertilization integuments and nucellus.....	68
11. Fluorescence micrograph of detached ovule penetrated by pollen tube 24 hrs. post-pollination <u>in vitro</u>	68
12. Light micrograph of longitudinal section through degenerate and persistent synergids 26 hrs. post-pollination <u>in vitro</u>	68
13. Light micrograph of longitudinal section through early zygote and persistent synergid 2 days post-pollination <u>in vitro</u>	68

FIGURE	PAGE
14. Light micrograph of longitudinal section through micropylar region of megagametophyte 2 days post-pollination <u>in vitro</u>	70
15. Light micrograph of longitudinal section through antipodals 2 days post-pollination <u>in vitro</u>	70
16. Light micrograph of longitudinal section through chalazal region of megagametophyte 2 days post-pollination <u>in vitro</u>	70
17. Light micrograph of longitudinal section through zygote.....	70
18. Light micrograph of a longitudinal section through two-celled proembryo 3 days post-pollination <u>in vitro</u>	72
19. Nomarski interference micrograph of free nuclear endosperm cell plates 3 days post-pollination <u>in vitro</u>	72
20. Light micrograph of free nuclear endosperm 3 days post-pollination.....	72
21. Light micrograph of oblique section through persistent antipodals 3 days post-pollination <u>in vitro</u>	72
22. Light micrograph of longitudinal section through thick walled hypostase 3 days post-pollination <u>in vitro</u>	72
23. Light micrograph of longitudinal section through embryo 4 days post-pollination <u>in vitro</u>	74
24. Light micrograph of longitudinal section through antipodals and hypostase 4 days post-pollination <u>in vitro</u>	74
25. Light micrograph of free nuclear endosperm cellularization 4 days post-pollination <u>in vitro</u>	74
26. Light micrograph of longitudinal section through embryo 4-5 days post-pollination <u>in vitro</u>	74
27. Light micrograph of longitudinal section through early globular embryo 6 days post-pollination <u>in vitro</u>	76

FIGURE	PAGE
28. Light micrograph of longitudinal section through integument, nucellus, and endosperm of seed 6 days post-pollination <u>in vitro</u>	76
29. Light micrograph of longitudinal section through integuments and endosperm of seed 8 days post-pollination <u>in vitro</u>	76
30. Light micrograph of endosperm from seed 8 days post-pollination <u>in vitro</u>	76
31. Light micrograph of longitudinal section through globular embryo 8 days post-pollination <u>in vitro</u>	76
32. Light micrograph of tangential section through endosperm adjacent to globular embryo 8-9 days post-pollination <u>in vitro</u>	78
33. Light micrograph of longitudinal section through globular embryo 9 days post-pollination <u>in vitro</u>	78
34. Light micrograph of longitudinal section through globular embryo 10 days post-pollination <u>in vitro</u>	78
35. Light micrograph of embryo-endosperm interface detail 10 days post-pollination <u>in vitro</u>	78
36. Light micrograph of mature endosperm 10 days post-pollination <u>in vitro</u>	80
37. Light micrograph of early stages of endosperm degradation 10 days post-pollination <u>in vitro</u>	80
38. Light micrograph of final stages of endosperm degradation 10 days post-pollination <u>in vitro</u>	80
39. Light micrograph of longitudinal section through embryo 12-13 days post-pollination <u>in vitro</u>	80
40. Light micrograph of longitudinal section through seed coat 20-22 days post-pollination <u>in vitro</u>	82
41. Light micrograph of longitudinal section through entire seed 22 days post-pollination <u>in vitro</u>	82

FIGURE	PAGE
42. Light micrograph of longitudinal section through cotyledon 24-25 days post-pollination <u>in vitro</u>	82
43. Light micrograph of longitudinal section through cotyledon 26 days post-pollination <u>in vitro</u>	82
44. Light micrograph of longitudinal section through embryonic shoot apex region 22 days post-pollination <u>in vitro</u>	84
45. Light micrograph of longitudinal section through embryonic root apex region 22 days post-pollination <u>in vitro</u>	84
46. Light micrograph of longitudinal section through embryonic root apex region in mature seed produced <u>in vitro</u>	84
47. Light micrograph of longitudinal section through embryonic shoot apex region in mature seed produced <u>in vitro</u>	84
48. Light micrograph of longitudinal section through embryonic root apex.....	86
49. Light micrograph of longitudinal section through mature seed coat.....	86
50. Light micrograph of longitudinal section through entire mature albuminous seed produced <u>in vitro</u>	86
51. Light micrograph of longitudinal section through two-celled proembryo 4 days after hand pollination <u>in vivo</u>	88
52. Light micrograph of oblique section through antipodals 4 days after hand pollination <u>in vivo</u>	88
53. Light micrograph of longitudinal section through micropylar end of seed 9-10 days after hand pollination <u>in vivo</u>	88
54. Light micrograph of longitudinal section through globular embryo 12 days after hand pollination <u>in vivo</u>	88
55. Light micrograph of longitudinal section through embryo 14-15 days after hand pollination <u>in vivo</u>	90

FIGURE	PAGE
56. Light micrograph of embryo-endosperm interface detail 14-15 days after hand pollination <u>in vivo</u> (same as in Fig. 55).....	90
57. Light micrograph of longitudinal section through embryonic shoot apex region in mature seed produced <u>in vivo</u>	90
58. Light micrograph of longitudinal section through embryonic root apex region in mature seed produced <u>in vivo</u>	90

CHAPTER ONE

INTRODUCTION

Successful test-tube fertilization in an angiosperm was first reported in Papaver somniferum L. by Kanta, Rangaswamy, and Maheshwari (1962). The time of anthesis and anther dehiscence had to be determined in order to emasculate and bag flowers before pollen was shed. On the day of anthesis, bagged gynoecia were collected along with anthers that were just beginning to open. Using aseptic technique, placentae with intact ovules were cultured on a nutrient medium without exogenous hormones and dusted with mature pollen. Numerous pollen tubes formed on and around the placental explants resulting in penetration and fertilization of some of the ovules. Fertilized ovules enlarged, turned a mealy white, and eventually acquired characteristic seed coats in contrast to the shrunken and collapsed nonfertilized ovules. Internal development of seeds produced in vitro appeared to follow the pattern observed in seeds formed in vivo, although later developmental stages in vitro were accelerated and enhanced.

Work on in vitro fertilization was expanded to other members of the Papaveraceae and Solanaceae (Kanta and Maheshwari, 1963; Maheshwari and Kanta, 1964). When the in vitro versus in vivo systems were compared in Papaver somniferum, it was observed that fertilization was accomplished from 1-2 days earlier in vitro. In an attempt to refine technique and improve results, other experiments using Argemone mexicana L., Eschscholzia californica Cham., Nicotiana rustica L., and N. tabacum L.

suggested that the process of in vitro fertilization could be enhanced if the placentae were collected from bagged gynoecia 24 hours after anthesis and by supplementing the medium with casein hydrolysate. In all species tested, fertilization occurred with subsequent seed maturation. Radicle emergence from the seed coat was observed in some of the mature seeds of Papaver somniferum, Nicotiana rustica, and N. tabacum while still attached to the placentae. Seedlings were formed only after seeds had been subcultured on fresh medium. In contrast, germination of Eschscholzia californica seeds resulted in callus formation, although regenerants developed and eventually produced seedlings after the callus had been subcultured on fresh medium. The success achieved in these experiments prompted other researchers to attempt in vitro fertilization in other species such as Petunia violacea Lindl. (Shivanna, 1965) and Antirrhinum majus L. (Usha, 1965).

It had been suggested that in vitro fertilization techniques could prove useful to plant breeders by circumventing gynoecial incompatibility within certain genera or between different genera (Kanta et al., 1962). Rangaswamy and Shivanna (1967) confirmed self-incompatibility in Petunia axillaris (Lam.) B.S.P. by demonstrating the inability of tubes from self-pollen to reach the ovary in contrast to successful fertilization in cross-pollinated flowers. To test the usefulness of in vitro fertilization, pre-fertilization placental explants with intact ovules of Petunia axillaris were dusted with self-pollen and incubated. Numerous pollen tubes were produced resulting in fertilization and formation of viable seed as confirmed by germination tests (Rangaswamy and Shivanna, 1967). Zenkteler (1967) attempted to induce intra-generic and inter-generic hybridization between members of the Caryophyllaceae. For all experiments,

pre-fertilization placentae with intact ovules were dissected from Melandrium album Mill. gynoecia. Individual placental explants were dusted with Melandrium album, M. rubrum, Silene schafta, S. tatarica, and Dianthus carthusianorum pollen respectively. Pollen germination and fertilization occurred in all cultures and embryo dissections from 14 day old seeds indicated normal development. Due to technical problems, mature seeds were obtained from only those cultures dusted with Melandrium album, M. rubrum, and Silene schafta pollen. Embryos dissected from these mature seeds were subcultured and eventually developed into seedlings that gave rise to new sporophytes capable of undergoing flower induction. Hybridization between species belonging to two different families was also attempted by Zenkteler (1970) using in vitro fertilization techniques. When ovules of Melandrium album were dusted with Datura stramonium pollen, a two-celled proembryo and endosperm nuclei developed as a result of successful fertilization, although the percentage of seed set was low. The proembryo eventually degenerated and the endosperm failed to develop beyond the 25 nuclei stage. The only explanation offered by Zenkteler (1970) was related to differences in ploidy between donor species. These experiments illustrate the potential usefulness of in vitro fertilization techniques to plant breeders interested in either hybridization or in circumventing certain self-incompatibility barriers to induce sexual production of diploid seedlings.

There have also been studies designed to alter various factors that may affect the in vitro fertilization system in Nicotiana tabacum. Experiments by Balatková and Tupý (1968) were designed to determine the fertilization potential of pre-existing pollen tubes before and after generative cell mitosis. It was determined that gamete formation in

N. tabacum occurred between 10-18 hours after pollen germination; therefore, pollen tubes cultured 8 hours and 20 hours were tested. Pre-fertilization placental explants were incubated in direct association with the pre-cultured pollen tubes which resulted in the subsequent formation of seeds in both the 8 hour and 20 hour old pollen tube cultures. In other experiments, Balatková and Tupý (1972) observed a retardation of post-fertilization in vitro development when large quantities of pollen were dusted over placental explants even though the culture medium was supplemented with casein hydrolysate. Restriction of growth due to numerous pollen tubes was considered as a possible explanation for the developmental retardation which prompted Balatková and Tupý (1972) to restrict pollen deposition to one area on the placenta. A higher percentage of seeds per placenta was obtained as a result of the localized pollination. Although there was no observable difference between cultures reared in diffuse light and those in the dark, seed set was increased when placentae were pollinated and cultured 1-3 days after anthesis in contrast to a substantial deterioration of cultures made 5 days after anthesis (Balatková and Tupý, 1972).

More recently, seeds of Narcissus pseudonarcissus L. c.v. Carlton formed in vitro failed to germinate even when subcultured or after treatment with Knopf's nutrient solution. Balatková et al. (1977) at first suggested that Narcissus seeds produced in vitro were not viable. This was shown not to be the case by Balatková et al., (1977) who reported that germination and seedling establishment took place only after the seeds had been sown in soil. Fertilization and seed development in Narcissus occurs in the early spring during periods of relatively low temperatures which suggested to Balatková et al. (1977) that these

developmental processes may be adapted to lower temperatures. In vitro fertilization and seed development were induced and the cultures incubated at 15C and 25C. The percentage of seed set was determined to be three times greater in cultures incubated at 15C than those at 25C. This evidence supported the hypothesis that fertilization and seed development are physiologically adapted to their natural environmental conditions (Balatková et al., 1977).

The Iceland Poppy (Papaver nudicaule L.), a garden variety perennial, was selected as the experimental organism for this study on the basis of (1) the previous in vitro fertilization success in other members of the Papaveraceae, (2) its greenhouse availability, and (3) because the processes of fertilization and seed formation have not been described for this species. The major objectives were (1) to characterize the morphological aspects of in vitro placental pollination and seed development and (2) to compare those observations with development in vivo on the light microscope level using conventional and modern histological and histochemical techniques.

CHAPTER TWO

POLLINATION

Materials and Methods

Flowers of Papaver nudicaule L. were emasculated and the gynoecia immediately bagged to prevent pollination on the day before anthesis. Intact placentae were dissected out of unpollinated gynoecia 1-3 days after anthesis. Pollen was aseptically collected from dehiscing anthers and dusted over and around the placental strips which were then cultured on modified Nitsch's growth medium at 23C (Appendix Two). Ovules were removed from placental explants at 15, 24, 31, and 48 hours post-pollination in vitro, fixed in buffered 3% glutaraldehyde for 3 hours, rinsed in 2 changes of phosphate buffer for 1 hour, post-fixed in buffered 2% osmium tetroxide for 2 hours, and rinsed a final time in phosphate buffer all at pH 6.8. Following dehydration in an ethanol series, the ovules were embedded in low viscosity resin (Spurr, 1969) (Appendix One). Intact placentae were fixed and dehydrated as previously described 15 hours after pollination, critical point dried, coated with gold and viewed with a Cambridge Stereoscan 150 scanning electron microscope. Some ovules removed from explants 24 and 31 hours in culture were fixed in buffered 3% glutaraldehyde for 3 hours, rinsed in phosphate buffer for 1 hour, treated with aniline blue for 15 minutes, and viewed in a depression slide using fluorescence microscopy to detect pollen tube

callose (Jensen, 1962). Ovules that had been penetrated by pollen tubes were post-fixed, dehydrated, and embedded.

Sections (0.5-1.0 μ m) of plastic embedded ovules were made using a Reichert OM U₂ ultramicrotome, mounted on autoradiography slides (Jensen, 1962), and stained with methylene blue (adapted from Suzuki, 1963) for general observation. Selected sections were treated with 0.5% 2,4-dinitrophenylhydrazine in 15% acetic acid as an aldehyde block prior to staining with periodic acid-Schiff's reagent to localize insoluble polysaccharides (Feder and O'Brien, 1968) and then were stained with aniline blue black to identify protein (Fisher, 1968) (Appendix One). A Zeiss Photomicroscope II was used for all light microscope observations.

Pre-fertilization Ovule

General morphology

The gynoecia of Papaver nudicaule L. are unilocular, multicarpellate structures that may contain several hundred ovules borne on as many as eight parietal placentae. Ovules range from 0.5mm-1.0mm in width and from 1.0mm-1.75mm in length with the micropyle oriented toward the base of the gynoecium. As in other members of the Papaveraceae (Corner, 1976), ovules of P. nudicaule L. are bitegmic, crassinucellate, and attached to the placenta by a pedestal-like funiculus. The micropyle formed by both integuments is directed toward the base of the funiculus and, therefore, the ovules may be described as campylotropous (Foster and Gifford, 1974).

Integuments

Outer integument -- The outer epidermis is composed of large, rectangular, thin walled, highly vacuolate cells that contain starch. Smaller, thin walled cells elongated parallel to the longitudinal axis of the ovule constitute the inner epidermis. In contrast to the outer epidermis, the cytoplasm of the inner epidermis is denser and also contains starch (Fig. 10).

Inner integument -- The outer epidermis is a narrow layer of thin walled, highly vacuolate cells that are elongated parallel to the ovular longitudinal axis and do not contain starch. Cells of the mesophyll layer are large, rectangular, thin walled, highly vacuolate, and also lack starch. In contrast, the inner epidermis is a layer of small, thin walled cells that are elongated perpendicular to the ovular longitudinal axis. These cells feature prominent vacuoles surrounded by dense cytoplasm, that may contain starch (Fig. 10).

Although Papaveraceous ovules are bitegmic, the number of layers composing each integument differs between genera (Corner, 1976). Earlier studies on the genus Papaver reported that the outer integument is two layers thick in contrast to the inner integument which has three layers (Meunier, 1891; Röder, 1958). These earlier observations are similar to those made in P. nudicaule.

Nucellus

The nucellus at the micropylar end of the Papaver nudicaule ovule is composed of cells that are small with thin walls and relatively large nuclei (Fig. 5,6). The cytoplasm contains numerous small vacuoles,

stains more intensely than neighboring integument cells, and also contains starch. A well developed micropylar nucellus is common among members of the Papaveraceae. In both Argemone mexicana and Eschscholzia californica, there are modified micropylar nucellar cells, the epistase, near the megagametophyte developing thick walls and containing dark staining substances (Sachar, 1955; Sachar and Ram, 1958). The epistase is absent in Dendromecon rigida (Berg, 1967) as well as in Papaver nudicaule.

Nucellus surrounding the megagametophyte is approximately 2-3 cell layers thick (Fig. 10). These cells are larger and stain less intensely than the micropylar nucellus. Nuclei are large and the cytoplasm is highly vacuolate featuring numerous starch containing plastids. This portion of the nucellus is eventually destroyed and replaced by the expanding megagametophyte.

The massive chalazal nucellus features a zone of degenerating cells encompassing several cell layers adjacent to the megagametophyte wall near the antipodals and a zone of intact cells extending toward the funiculus (Fig. 7). The degenerating cells contain numerous starch containing plastids. These highly vacuolate cells become more disorganized until they are disrupted and eventually crushed by megagametophyte expansion. The intact nucellar cells are less vacuolate, smaller, and contain little starch.

A column of small, contiguous cells 2-3 layers thick connects the region close to the terminus of the funicular vascular strand in the intact chalazal nucellus with the base of the antipodals (Fig. 7). These modified nucellar cells, the hypostase, have thick PAS positive staining cell walls and often contain dark staining substances (Corner,

1976) (Fig. 22). It has been suggested that the hypostase facilitates translocation of metabolites into the megagametophyte (Masand and Kapil, 1966). Coe (1954) conducted autoradiographic studies on Zephyranthes (Amaryllidaceae) ovules and reported a high level of $^{14}\text{CO}_2$ localization in the chalazal nucellus in contrast to a low incorporation of $^{14}\text{CO}_2$ in the hypostase. The hypostase does not appear to function in metabolite translocation in Zephyranthes ovules. The hypostase is a common component of Papaveraceous ovules (Corner, 1976), but hypostase significance, if any, remains unclear.

Megagametophyte

The mature megagametophyte of Papaver nudicaule is composed of seven cells with eight nuclei. An egg apparatus consisting of two synergids and an egg arranged in a triadic juxtaposition resides in the micropylar region of the megagametophyte. The chalazal region of the megagametophyte is occupied by two polar nuclei and three antipodals that are also arranged in a triadic juxtaposition. Megagametophyte development in the Papaveraceae is of the Polygonum-type (Davis, 1966).

Synergids

In Papaver nudicaule, synergids are equal in size and are broader at the micropylar end than at the chalazal end (Fig. 5). Each synergid is surrounded by a PAS positive staining wall as in Capsella bursa-pastoris (Schulz and Jensen, 1968a), Hordeum vulgare (Cass and Jensen, 1970), and Helianthus annuus (Newcomb and Steeves, 1971). In Capsella and Helianthus, however, the chalazal portion of the synergid wall is thin, irregular, and permits contact between synergid-central cell membranes

(Schulz and Jensen, 1968a; Newcomb, 1973a). Chalazal walls are absent in synergids of Gossypium hirsutum (Jensen, 1965a), Zea mays (Diboll and Larson, 1966), Petunia hybrida (Van Went, 1970a), Eschscholzia californica (Negi, 1974), and Proboscidea louisianica (Mogensen, 1978). Mogensen (1972) reported that synergids of Quercus gambelii lack chalazal walls prior to fertilization, but complete walls develop after fertilization. Each synergid of Papaver nudicaule also features a PAS positive staining filiform apparatus that appears to be more massive than those found in other species (Jensen, 1965a; Schulz and Jensen, 1968a; Cass and Jensen, 1970; Mogensen, 1972; Negi, 1974). The filiform apparatus is confluent with the micropylar region of the synergid wall and forms numerous finger-like structures that project into the synergid (Fig. 5). This network of projections increases the surface area of the plasmalemma facilitating translocation of materials in and out of the synergid much like a transfer cell (Gunning and Pate, 1969; Pate and Gunning, 1972).

The nucleus with its single nucleolus is situated near the common wall between sister synergids in close proximity to the filiform apparatus. A large chalazal vacuole restricts the cytoplasm to the lower two-thirds of the synergid. The cytoplasm contains PAS positive staining granules as do the synergids of Stellaria media (Pritchard, 1964) and Gossypium hirsutum (Jensen, 1965a) which may indicate metabolic activity.

Egg

The pear-shaped egg is wider at the chalazal end than at the micropylar end and measures 52 μ m in length and 37 μ m at the widest point (Fig. 6). The entire egg is surrounded by a PAS positive staining wall

as in the egg of Capsella (Schulz and Jensen, 1968b) and Hordeum (Cass and Jensen, 1970). In Helianthus (Newcomb, 1973a), the thick micropylar wall of the egg gradually becomes thin and irregular resulting in a "partial wall" toward the chalazal end. The egg of Eschscholzia has a thick wall at both the micropylar and chalazal ends (Negi, 1974). In the middle one-third of the Eschscholzia egg, however, the wall is thin and irregular allowing direct contact between synergid-egg membranes. In contrast, the chalazal portion of the egg wall is absent in Gossypium (Jensen, 1965b), Zea (Diboll and Larson, 1966), Petunia (Van Went, 1970b), and Quercus (Mogensen, 1972).

The chalazal two-thirds of the egg is dominated by a large vacuole that confines most of the cytoplasm to the micropylar one-third. The nucleus is approximately 12 μ m in diameter and lies just below the vacuole (Fig. 6). The cytoplasm contains starch as do the eggs of other genera such as Gossypium (Jensen, 1965b), Capsella (Schulz and Jensen, 1968b), Hordeum (Cass and Jensen, 1970), and Eschscholzia (Negi, 1974). Polarity of the egg of Papaver nudicaule as expressed by a micropylar nucleus and chalazal vacuole is characteristic for other Papaveraceous eggs such as Argemone mexicana (Sachar, 1955), Eschscholzia californica (Sachar and Ram, 1958), and Dendromecon rigida (Berg, 1967). Negi (1974), however, reported that the egg of Eschscholzia has a chalazal nucleus and micropylar vacuole. The latter type of egg polarity is presumably more common among angiosperms (Maheshwari, 1950; Raghavan, 1976).

Central Cell

The central cell is the largest cell of the Papaver nudicaule megagametophyte. The PAS positive staining central cell wall is evenly

thickened and appears to be continuous with the cell walls of the egg apparatus in the micropylar region as well as the three antipodals in the chalazal region. In genera such as Gossypium (Jensen, 1965a,b) and Zea (Diboll and Larson, 1966) where chalazal walls are absent from synergids and egg, central cell wall is also absent from adjacent positions resulting in direct membrane contact between egg apparatus and central cell. Schulz and Jensen (1968a,b) reported that even though cells of the egg apparatus in Capsella have common walls with the central cell, the walls contain irregularities and gaps which permit either direct membrane contact or place membranes in close proximity to one another. In Eschscholzia (Negi, 1974), the common wall between the central cell and the synergids was lacking in contrast to a thick common wall between central cell and egg.

Although the most commonly observed location for the polar nuclei in most angiosperms is in the vicinity of the egg apparatus (Maheshwari, 1950), the polar nuclei of Papaver nudicaule are located in the chalazal end of the central cell adjacent to the antipodals (Fig. 8). Chalazal polar nuclei have been reported in other Papaveraceous megagametophytes (Sachar, 1955; Berg, 1967), except in Eschscholzia where the polar nuclei lie adjacent to the egg apparatus (Sachar and Ram, 1958; Negi, 1974). The time of polar nuclei fusion varies between genera. The polar nuclei of Gossypium (Jensen, 1965b), Zea (Diboll and Larson, 1966), and Hordeum (Cass and Jensen, 1970) begin to fuse prior to fertilization, but complete the process after fertilization. Van Went (1970b) reported that polar nuclei of Petunia can fuse either before or after fertilization in contrast to Capsella (Schulz and Jensen, 1968b, 1973) and Eschscholzia (Negi, 1974) where fusion of polar nuclei takes place before fertilization.

In fertilized ovules of Papaver nudicaule, the polar nuclei normally fuse after pollen tube penetration of the megagametophyte. The polar nuclei of unfertilized ovules eventually fuse to form a large chalazal secondary nucleus with a single nucleolus. The majority of the vacuolate central cell cytoplasm is situated around the secondary nucleus near the antipodals (Fig. 8). A large central vacuole confines the remaining cytoplasm to the periphery of the central cell. The cytoplasm stains lightly for protein and contains starch as do the central cells of other species (Jensen, 1965b; Diboll and Larson, 1966; Cass and Jensen, 1970; Schulz and Jensen, 1973). The overall expansion of the megagametophyte may indicate that the central cell of P. nudicaule is metabolically active.

Antipodals

Three large antipodals join together in the vicinity of the hypostase at the chalazal end of the mature megagametophyte of Papaver nudicaule. Each cell is surrounded by a PAS positive staining wall featuring an elaborate network of branching wall ingrowths at the antipodal-nucellus interface (Fig. 7). The wall projections are less massive than synergid filiform apparatuses and appear similar to those attributed to transfer cells that serve to increase the surface area of the plasmalemma (Gunning and Pate, 1969; Pate and Gunning, 1972). The micropylar one-third of each antipodal is occupied by a large vacuole. Situated in the chalazal two-thirds of each cell is a large nucleus that is surrounded by dense cytoplasm. Antipodals reflect the mirror image of the polarity expressed in the cells of the egg apparatus.

Polarized antipodals are common in certain genera of the Papaverales. Huss (1906) surveyed antipodal morphology in Dicentra spectabilis, Corydalis nobilis, Fumaria officinalis, and several species of Papaver. Antipodals from these plants were shown to have large nuclei and associated cytoplasm mostly restricted to the chalazal portion of the cell by a large micropylar vacuole or vacuoles. The more recent antipodal morphological reports on Argemone mexicana (Sachar, 1955), Eschscholzia californica (Sachar and Ram, 1958), and Dendromecon rigida (Berg, 1967) are in agreement with the earlier studies. An ultrastructural investigation by Negi (1974) of the antipodals of Eschscholzia revealed that ingrowths also develop from the wall adjacent to the degenerating nucellus. The large nucleus of Eschscholzia antipodals is presumably polyploid from endomitotic activity, but its significance to antipodal function, if any, remains unclear. Negi (1974) concluded that Eschscholzia antipodals are metabolically active based on the presence of large nuclei, wall ingrowths, and a full complement of cytoplasmic organelles. If this conclusion is correct, the wall ingrowths and large nuclei of Papaver nudicaule antipodals would suggest a similar degree of cellular activity.

Pollination Events

Pollen germination -- Pollen that lands on the surface of ovules or placenta begins to germinate within 20-30 minutes. Pollen that lands directly on the growth medium begins to germinate after one hour. These observations are in agreement with those of Kanta et al. (1962) and Kanta and Maheshwari (1963) for Papaver somniferum. The pollen of

P. somniferum germinates within 15 minutes after contact with the ovular surface in contrast to the one hour needed for germination by the pollen on the growth medium.

Pollen tube growth in vitro is similar to the pattern of growth followed by some pollen tubes in vivo. Cass and Jensen (1970) reported that in vivo pollen tubes of Hordeum first come into contact with the chalazal end of the ovule and then proceed to grow along the ovular surface toward the micropyle. In Persea, pollen tubes enter the locule, grow along the inner ovarian wall, around the funiculus, and make contact with the micropyle (Sedgley, 1979). In Papaver nudicaule, most pollen tube growth in vitro is random; however, there is directional growth toward the micropyle from those pollen grains in direct contact with ovules or placenta (Fig. 3,9). Aniline blue fluorescence reveals a callose-like carbohydrate component to the pollen tube wall of P. nudicaule and the formation of internal callose plugs (Fig. 11). Callose has been reported in the pollen tubes of many species and may serve either as a storage carbohydrate or add strength to the wall (Stanley, 1971; Herth et al., 1974). Callose plugs presumably confine cytoplasmic streaming to the area of elongation (Stanley and Linskens, 1974). Scanning electron microscopy demonstrates the fibrillar nature of external pollen tube wall morphology (Stanley and Linskens, 1974; Herth et al., 1974) and where internal callose plugs have formed (Fig. 4).

Path of the pollen tube -- In Papaver nudicaule, a pollen tube enters the ovule through the micropyle and grows along the micropylar canal until contact is made with the nucellus. The pollen tube proceeds intercellularly through the nucellus emerging near the nucellus-megagametophyte interface at the base of the two synergids. The pollen tube enters

the megagametophyte by growing into the filiform apparatus of one or the other synergid. Synergid penetration occurs approximately 24 hours after pollination in vitro. The synergid that receives the pollen tube stains intensely obscuring internal detail.(Fig. 12).

In plants such as Gossypium hirsutum (Jensen and Fisher, 1968), Hordeum vulgare (Cass and Jensen, 1970), and Proboscidea louisianica (Mogensen, 1978) one of the two synergids begins to degenerate before the pollen tube enters the megagametophyte. In plants such as Petunia hybrida (Van Went, 1970c) and Eschscholzia californica (Negi, 1974), it appears that rapid synergid degeneration is a direct result of pollen tube penetration and discharge. Degeneration of synergids in Papaver nudicaule is accompanied by the presence of a penetrating pollen tube. Unfertilized ovules that were pollinated also show no evidence of synergid degeneration. These observations indicate that in P. nudicaule, the synergids may remain intact until one is penetrated by a pollen tube. If this mode of megagametophyte entry is correct, then P. nudicaule resembles another member of the Papaveraceae in this respect, Eschscholzia californica (Negi, 1974). Pollen tube growth terminates in the degenerate synergid of Papaver nudicaule where the gametes are presumably discharged as in other angiosperms (Jensen and Fisher, 1968; Schulz and Jensen, 1968a; Cass and Jensen, 1970; Negi, 1974; Mogensen, 1972, 1978). Events involving the fusion of egg with sperm and sperm with polar nuclei were not observed in P. nudicaule presumably as a result of the speed of the overall process (Maheshwari, 1950).

Discussion

Maheshwari (1950) reported that the antipodals of many angiosperms appeared to be metabolically active cells, but their function was unknown at the time. Antipodals have been implicated in the nutrition of angiosperm megagametophytes in general, but especially in certain members of the Gramineae and Papaveraceae (Brink and Cooper, 1944; Masand and Kapil, 1966). In Zea mays, numerous antipodals occupy the chalazal end of the megagametophyte (Diboll and Larson, 1966). Wall projections develop in antipodals from the center of the cell mass as well as in antipodals immediately adjacent to the chalazal nucellus that presumably increase plasmalemma surface area. Diboll and Larson (1966) also observed that some antipodals fail to form complete walls which results in direct membrane contact between neighboring cells and that the cytoplasm contains an abundance of mitochondria, dictyosomes, and endoplasmic reticula. As previously discussed, the antipodals of Eschscholzia californica also contain a full complement of organelles and possess extensive chalazal wall ingrowths (Negi, 1974). The structural observations in both Zea mays (Diboll and Larson, 1966) and Eschscholzia californica (Neig, 1974) support the proposed nutritive function of antipodals.

The structural and developmental relationships between the nucellus and the antipodals of Aesculus woerlitzensis Koehne led List and Steward (1965) to hypothesize the occurrence of metabolite translocation from the nucellus into the antipodals and from antipodals into the rest of the megagametophyte. Supporting structural evidence is based on a well developed chalazal nucellus that undergoes degradation at the

interface between chalazal megagametophyte wall and adjacent nucellus accompanied by hypostase development at the base of the antipodals. There are numerous examples in other angiosperms of intraovular relationships between chalazal structures that may function in the absorption, storage, and/or translocation of metabolites (Masand and Kapil, 1966; Raghavan, 1976). In Eschscholzia californica (Papaveraceae), a well developed hypostase is situated between the base of the antipodals and where the ovular vascular supply terminates in the chalazal nucellus. Nucellus in the vicinity of the hypostase-antipodal interface undergoes degradation which led Negi (1974) to suggest the existence of a nutritional relationship between structural components of the megagametophyte. Morphological evidence from Papaver nudicaule also suggest a major pathway of nutrient flow into the megagametophyte through the chalazal region. The funicular vascular strand terminates in the intact chalazal nucellus in the vicinity of the hypostase. The hypostase may bridge translocation from the intact nucellus to the base of the antipodals. The starch filled nucellus adjacent to the antipodal chalazal wall in-growth breaks down and may function as a nutrient source that is readily available to the antipodals. Structurally the antipodals of P. nudicaule resemble transfer cells (Gunning and Pate, 1969; Pate and Gunning, 1972) and may represent sites for accumulation and/or active transport of metabolites into the central cell.

Ultrastructural studies of central cell cytoplasm in some angiosperms have led researchers to conclude that central cells are metabolically active cells (Jensen, 1965b; Van Went, 1970b; Schulz and Jensen, 1973; Newcomb, 1973a). Some central cell walls develop projections presumably to maximize translocation of materials in or out. In

Helianthus annuus, wall projections are located at the micropylar end of the central cell (Newcomb and Steeves, 1971). Newcomb (1973a) suggested that wall projections may play an important role in both preparing the central cell for endosperm development and supplying the egg apparatus with needed metabolites. Negi (1974) found the central cell cytoplasm of Eschscholzia californica to be devoid of starch, but wall projections develop in the vicinity of the egg apparatus prior to fertilization. Negi (1974) suggested that the wall projections are crucial to the nutrition of the egg apparatus as the megagametophyte reaches maturity. The central cell of Papaver nudicaule does not develop wall projections, but probably functions as a nutrient "sink" during megagametophyte maturation.

Jensen (1965a) studied the fine structure and histochemistry of Gossypium hirsutum synergids. Each synergid possesses a filiform apparatus consisting of internal micropylar wall projections that increase the surface area of the plasmalemma. Jensen (1965a) reasoned that the numerous mitochondria and abundant endoplasmic reticula observed in close association with the filiform apparatuses probably provide the energy needed for possible active transport and an internal transport system respectively. Storage compartments within the synergids could also be provided for by the numerous dictyosomes observed in the vicinity of the endoplasmic reticula. As in Stellaria media (Pritchard, 1964), Gossypium synergids were shown to contain starch (Jensen, 1965a). The starch is restricted to large numbers of plastids near the periphery of the filiform apparatuses. Such observations led Jensen (1965a) to argue in favor of an active role for synergids in the nutrition of the egg as well as the central cell. Fine structural components of synergids

in Zea mays (Diboll and Larson, 1966; Diboll, 1968) and Capsella bursa-pastoris (Schulz and Jensen, 1968a) suggest metabolic activity which may indicate some involvement in the translocation and/or accumulation of metabolites. In Papaver nudicaule, the presence of starch and well developed filiform apparatuses provide reasonable morphological and histochemical evidence for suggesting synergid participation in egg and central cell nutrition, but more evidence is needed.

Synergids have also been suggested as the source of erotropic substances (Machlis, 1972) responsible for guiding pollen tubes into the ovule and eventually into the megagametophyte (Van der Pluijm, 1964; Jensen, 1965a). In some angiosperms, the degeneration of one synergid prior to pollen tube arrival at the megagametophyte and penetration of that synergid by the pollen tube suggest that synergids may attract the pollen tubes (Jensen and Fisher, 1968; Cass and Jensen, 1970; Mogensen, 1978). These studies imply that substances from the degenerating synergid are released into the micropylar region of the ovule and are detected by the pollen tube. The pollen tube presumably follows a gradient of the erotropic substances to the megagametophyte and eventually penetrates and discharges its contents into the degenerate synergid. There are other flowering plants in which neither synergid degenerates until after the pollen tube has actually penetrated one or the other of them (Van Went, 1970c; Mogensen, 1972; Negi, 1974). In these studies, attention is focussed on the filiform apparatus as the outlet for erotropic substances produced in the synergids or in the central cell. In most cases where synergids are present, pollen tubes enter the megagametophyte by growing through the filiform apparatus into a synergid whether synergid degeneration occurs before or as a result of pollen tube

penetration (Jensen and Fisher, 1968; Schulz and Jensen, 1968a; Cass and Jensen, 1970; Van Went, 1970c; Newcomb, 1973b; Negi, 1974; Mogensen, 1972, 1978).

The chemical nature of pollen tube guidance is unclear; however, one possibility is the calcium ion (Brewbaker and Kwack, 1963). Mascarenhas and Machlis (1962) detected a calcium ion gradient in the gynoecial tissues of Antirrhinum majus. The concentration of calcium ions increased from the stigmatic surface down the style toward the ovules. This observation led Mascarenhas and Machlis (1962) to propose that calcium ion gradients may be involved in directing pollen tube growth toward the ovules. It was discovered, however, that the placentae of both Antirrhinum majus (Mascarenhas, 1966) and Oenothera longiflora (Glenk et al., 1971) contain twice as much calcium as their ovules. Mascarenhas (1966) concluded that calcium ions may be involved in directing pollen tube growth down the style, but other substances are probably responsible for guiding pollen tubes into the ovules. There is no information available concerning calcium ion concentrations in the gynoecial tissues of Papaver nudicaule, but if, as in Antirrhinum (Mascarenhas, 1966) and Oenothera (Glenk et al., 1971), the placentae contain higher calcium concentrations than the ovules, other erotropic substances could be involved since there is directional pollen tube growth toward the micropyle in vitro. It is possible that the synergids of Papaver nudicaule may also be the source of erotropic substances released into the micropylar end of the ovule via the filiform apparatuses that establish a gradient to attract the pollen tube into the ovule and subsequently into the megagametophyte, but no experimental evidence to support this notion is available.

Egg apparatuses of angiosperms such as Gossypium hirsutum (Jensen, 1965a,b), Zea mays (Diboll and Larson, 1966), Petunia hybrida (Van Went, 1970a,b), Quercus gambelii (Mogensen, 1972), Helianthus annuus (Newcomb, 1973a), and Proboscidea louisianica (Mogensen, 1978) presumably do not possess major restrictive physical barriers to sperm transfer from synergid to egg or from synergid to central cell. In these plants, the lack of chalazal end walls in synergids and egg provide direct membrane contact between cells of the egg apparatus and the central cell. In Capsella bursa-pastoris (Schulz and Jensen, 1968a,b) the cells of the egg apparatus are surrounded by wall material, but there is an opening in the common wall between synergid and egg. This opening is usually found in the vicinity of the pollen tube discharge and appears similar in diameter to the sperm. The synergids of Eschscholzia californica do not have chalazal end walls, but the egg cell does (Negi, 1974). There is membrane contact between synergid and central cell which could facilitate sperm transfer to the polar nuclei and a wall free area of the egg which also results in membrane contact between synergid and egg. Negi (1974) suggested that sperm transfer from synergid to egg is made in the region of direct membrane contact. The cells of the Papaver nudicaule egg apparatus are surrounded by PAS positive staining wall material. Fine structural studies may help elucidate a possible mechanism for sperm transfer from synergid to egg and central cell as well as provide evidence either for or against the proposed functions of synergids, central cell, and antipodals.

CHAPTER THREE

SEED DEVELOPMENT

Materials and Methods

To obtain seeds formed in vitro, pre-fertilization placental explants with intact ovules were dusted with pollen and incubated at 23°C on modified Nitsch's medium (Appendix Two). In vivo formed seeds were obtained by hand-pollinating pre-fertilization stigmata at the time of anthesis. The hand-pollinated flowers were allowed to continue development under greenhouse conditions (21-23°C) at the University of Alberta. Seeds at different developmental stages were collected from either placental cultures or from the greenhouse flowers and prepared for either paraffin or plastic microtechnique. Prior to embedding in "Paraplast-Plus" (m.p. 56-57°C), fertilized ovules were fixed in Craf solution overnight, washed in running water for 8 hours and dehydrated in an ethanol-tertiary butyl alcohol series (Johansen, 1940; Sass, 1958). For general observation, sections (10-12µm) were cut on a Spencer AO 820 rotary microtome, mounted on glass slides with Haupt's adhesive, and stained with safranin-fast green (Johansen, 1940). Ovules for plastic sectioning were fixed in buffered 3% glutaraldehyde for 3 hours, washed in two changes of phosphate buffer for 1 hour, post-fixed in buffered 2% osmium tetroxide for 2 hours, and washed again in phosphate buffer for 1 hour, all at pH 6.8. Dehydration was done in an ethanol series followed by embedding in low viscosity resin (Spurr, 1969) (Appendix One).

Plastic sections (0.5-1.0 μ m) were cut using a Reichert OM U₂ ultramicrotome, mounted on autoradiography slides (Jensen, 1962), and stained with either toluidine blue (Trump et al., 1961) or methylene blue (adapted from Suzuki, 1963) for general observation.

Limited histochemical procedures were carried out on plastic sections to localize and characterize major seed food reserves (Appendix One). Aniline blue black (Fisher, 1968) and Sudan black B (Bronner, 1975) were used to identify proteins and lipids, respectively. Sections to be treated with periodic acid-Schiff's reagent to detect insoluble polysaccharides were first subjected to a 0.5% solution of 2,4-dinitrophenylhydrazine in 15% acetic acid as an aldehyde blockade (Feder and O'Brien, 1968). Aniline blue fluorescence microscopy was utilized to reveal the presence of any callose-like material (Jensen, 1962).

To examine the possible influence of placental tissues on development, fertilized ovules were removed from their placentae at 4, 6, 8, 15 and 22 days post-pollination and transferred to fresh, modified Nitsch's growth medium. Subcultured ovules were incubated at 23C until each seed had been in culture a total of 26 days. Seeds were then processed for plastic embedding, sectioning, and observed as previously described. All observations were made with a Zeiss Photomicroscope II.

Post-fertilization Ovule In vitro

Embryogenesis

Zygote -- Transformation from egg to zygote occurs between 24 and 31 hours post-pollination and results in a decrease in cell size

accompanied by a reversal of cytoplasmic polarity. The zygote is approximately 34-36 μ m long and, in contrast to the egg, has a more uniform width of 24-25 μ m and is surrounded by a PAS positive staining wall (Fig. 13, 14, 17). Zygote organization in Papaver nudicaule features a chalazal nucleus surrounded by a concentration of cytoplasm and a micropylar end dominated by a large vacuole. Reversal of polarity in the zygote is in agreement with studies of other members of the Papaveraceae (Souéges, 1928; Sachar and Ram, 1958) as well as in other documented angiosperm studies (Schulz and Jensen, 1968b; Jensen, 1968; Ashley, 1972). There is a discrepancy as to the zygote polarity in Eschscholzia (Papaveraceae). Sachar and Ram (1958) maintained that the nucleus is chalazal, whereas, Negi (1974) insisted that the nucleus migrates to a micropylar position. The phenomenon of zygote shrinkage and reorganization has been thought to play a vital role in the orientation of subsequent cell division (Jensen, 1968; Raghavan, 1976). It was demonstrated that Hibiscus hybrid zygotes failed to undergo these changes. Hybrid zygotes underwent mitosis in approximately the same time frame as self-fertilized zygotes, but continued mitosis resulted in a clump of nondifferentiated cells. These data led Ashley (1972) to conclude that zygote shrinkage and cytoplasmic reorganization are essential to future differentiation of the embryo.

Jensen (1968) proposed that a reduction of plasmalemma and tonoplast areas concomitantly with a decrease in vacuole water content take place during the decrease in cell size from egg to zygote. Direct membrane degradation or conversion of plasmalemma and tonoplast into endoplasmic reticulum have been suggested as possible methods for decreasing membrane area, the latter supported by evidence from Gossypium (Jensen, 1968).

In Papaver nudicaule, the zygote nucleus is approximately 17-18 μ m in diameter and contains a single nucleolus (Fig. 13, 17). The dense cytoplasm surrounding the nucleus contains numerous starch containing plastids. Starch containing plastids have also been observed in zygotes of Capsella and Gossypium (Schulz and Jensen, 1968b; Jensen, 1968). The remaining chalazal and micropylar cytoplasm remain homogeneous. Unlike Capsella (Schulz and Jensen, 1968b), accumulation of dense staining material in the periphery of the micropylar vacuole of Papaver zygotes was not observed.

Proembryo -- The first division of angiosperm zygotes is usually transverse (Maheshwari, 1950). In Papaver nudicaule, the zygote divides transversely to form a two-celled proembryo approximately three days post-pollination in vitro (Fig. 18). The apical cell is smaller than the basal cell and appears to have denser cytoplasm, while the basal cell maintains the large micropylar vacuole. Both cells contain starch and the nuclei contain more than one nucleolus. Embryogeny in P. nudicaule is of the Solanad type as is common in the Papaveraceae (Davis, 1966). The basal cell divides transversely a second time followed by a similar division of the apical cell to form a filamentous four-celled proembryo. The basal cell retains the large micropylar vacuole while the derivatives of the apical cell appear to have denser cytoplasm. This mode of proembryo establishment has been described for other members of the Papaveraceae (Souéges, 1926, 1928, 1948, 1949a; Créte, 1957; Sachar and Ram, 1958), however, there is uncertainty about proembryo establishment in Argemone mexicana. Souéges (1949b) described the first division of the zygote of Argemone as vertical or oblique with subsequent divisions forming an irregular proembryo. Sachar (1955) observed

the occasional oblique division of the Argemone zygote, but found transverse divisions to be predominant. Crété (1956) defended the original description of an oblique plane of cell division. It was concluded that the orientation of division in zygotes of A. mexicana is variable and as a result the patterns of subsequent divisions of the two-celled proembryo are likewise variable (Sachar, 1956). Variations in the pattern of early development were not observed in Papaver nudicaule.

Early globular embryo -- The subapical cell of the filamentous proembryo of Papaver nudicaule is the first to undergo a vertical division followed by a similar division of the apical cell (Fig. 23,26). These two divisions mark the initial differentiation of the embryo proper from the suspensor. Subsequent vertical divisions produces a globular octet supported by a two-celled suspensor (Fig. 27). Staining intensity is more pronounced in the embryo proper when compared with the suspensor. The sequence of mitotic divisions followed in P. nudicaule to establish an embryo proper conforms to the pattern described for P. rhoeas L. and Roemeria violacea Medic. (Souéges, 1926, 1928, 1948). Other genera within the Papaveraceae, such as Eschscholzia and Dicranostigma, usually develop a multicellular filament with the first vertical division in the apical cell (Souéges, 1949a; Crété, 1957; Sachar and Ram, 1958).

Continued divisions in the embryo of Papaver nudicaule result in a multicellular suspensor and a globular embryo proper with distinct regions designated as contributors to various organs of the mature embryo (Fig. 31). The outermost layer of the young embryo will eventually form the protoderm. The upper region of the inner cells contributes to the epicotyl while the lower region of the inner cells contributes to the hypocotyl. Mitotic derivatives of the terminal cell of the suspensor,

the hypophysis, are incorporated into the embryonic root tip (Maheshwari, 1950). This general developmental scheme for the future organization of the mature embryo is similar to that described for P. rhoeas. (Souéges, 1926, 1928). Suspensor vacuolation increases from the hypophysis to the basal cell.

Late globular embryo -- Nine days after in vitro pollination, a large globular embryo is formed (Fig. 33). The incipient protoderm, cells of the inner region, and derivatives of the hypophysis exhibit similar cytoplasmic staining characteristics and starch. The entire embryo proper stains more intensely than the highly vacuolate suspensor which also contains starch.

Changes in the globular Papaver embryo are observed after 10 days in culture (Fig. 34). The outer tangential walls of the entire incipient protoderm are crenulated (Fig. 35). Although the cells continue to possess starch, cytoplasm staining intensity is greater than the rest of the embryo. Many cells of the inner regions are more elongate and their vacuolate cytoplasm contains relatively little, if any, starch. In comparison, derivatives of the hypophysis do contain starch and possess the occasional vacuole, but stain less intensely. Suspensor cytoplasm remains less dense in relation to the embryo proper, but continues to accumulate starch.

Cotyledon initiation -- The globular embryo of Papaver nudicaule undergoes substantial cell division and elongation resulting in an elongated embryonic axis with a flattened distal surface similar to that described for Downingia (Kaplan, 1969). Cotyledon initiation results from localized mitotic activity that produces two primordia. As cotyledon primordia begin to develop, an epicotyl dome is formed.

The degree of epicotyl convexity depicted in P. rhoeas by Souéges (1928) was not observed in P. nudicaule. Differentiation of the three primary meristems and their derivatives also begins at this stage (Fig. 39). The distinctive uniseriate protoderm is maintained by anticlinal divisions in contrast to the nonvacuolate cortical ground meristem of the hypocotyl. Incipient procambial cells are elongate showing varying degrees of vacuolation. The longitudinal axis of the provascular cylinder is delimited by the future shoot and root apices. Cells in the region of the shoot apex appear larger, less dense, and more vacuolate in contrast to the surrounding tissue. The more distince root apex becomes organized into well defined tiers. The overall morphology of the embryo at this stage is comparable with the description of P. rhoeas (Souéges, 1928).

Aggregation of the protein bodies in Papaver nudicaule appears to be restricted to suspensor, ground meristem, and protoderm, but with a definite concentration in the cotyledon primordia (Fig. 39). Cotyledons stain more intensely than the rest of the embryo and feature crenulated outer tangential walls (Fig. 41,42). Crenulations are maintained as development continues, but become restricted to the cotyledon tips during later stages of embryo differentiation (Fig. 43,50). The bulk of each cotyledon is made up of ground tissue. As the cotyledons elongate, the ground tissue is highly vacuolate; however, the ground tissue becomes increasingly less vacuolate as cotyledons mature and exhibit increased protein, carbohydrate, and lipid content. Differentiation of the procambium from the main provascular core into the cotyledons of P. nudicaule is acropetal as has been observed in other angiosperms (Cutter, 1971; Esau, 1977).

Epicotyl -- As the cotyledons elongate, the epicotyl of Papaver nudicaule is characterized by the presence of 2-4 cells which are larger and stain less intensely than surrounding cells. Large cells centrally located in the epicotyl dome of P. rhoeas were identified as stem cortical initials by Souéges (1928). As development continues in P. nudicaule, the central zone of the dome increases in cell number and becomes more discernible from other epicotyl cells and the subtending procambium (Fig. 41,44). These randomly arranged large apical cells contain starch and are highly vacuolate appearing to be relatively undifferentiated. In the mature embryo, the apex is organized into two regions. The first region consists of 1 to 2 distinct outer cell layers subtended by the second region which is a central zone of randomly arranged cells (Fig. 47). Large, vacuolate cells with large nuclei are identifiable in both shoot apical zones. Organization of the shoot apex in mature embryos of P. somniferum (Bersillon, 1955) is similar to the arrangement in the P. nudicaule embryonic shoot apex.

The vegetative apex of P. somniferum has been interpreted in terms of Buvat's (1952) "waiting meristem" theory in which a region of quiescent cells becomes mitotically active only during the transition to a reproductive apex. Bersillon (1955) also maintained that all zones characterized in the adult vegetative apex by this theory could be recognized in the embryonic apex. For morphological comparison I suggest that the vegetative apex of Papaver somniferum can be described as consisting of a tunica and a corpus and that the embryonic apex would reflect that organization. The tunica-corpus theory proposed by Schmidt (1924) states that the tunica is represented as the outermost layer or layers whose primary plane of cell division is anticlinal. The

corpus central cell mass is directly beneath the tunica. Both the tunica and corpus are presumed to possess their own initials which are larger, have larger nuclei, are more vacuolate, and stain less intensely when compared to other cells in the tunica and corpus (Fahn, 1974; Esau, 1977). Tunica-corpus organization has also been described in shoot apices of other mature angiosperm embryos. Miller and Wetmore (1945) described the embryonic shoot apex of Phlox drummondii as composed of a single tunica layer subtended by the corpus. In Garrya elliptica embryos, there is a single tunica layer, but in some preparations Reeve (1948) found that the embryonic tunica showed variation and could be composed of more than one layer. The embryonic apex of Pisum sativum was found to exhibit two very distinct tunica layers (Reeve, 1948). In Papaver nudicaule, the two outer layers of the embryonic shoot apex may also represent the immature tunica and the underlying central zone the immature corpus.

Hypocotyl -- As previously noted, the future root apex is already organized into tiers at the time of cotyledon initiation (Fig. 39). As the embryonic axis elongates, these meristematic tiers and their derivatives become even more discernible from one another (Fig. 45) and upon embryo maturation there are three distinct layers (Fig. 46,48). On the basis of morphology alone, one may employ Hanstein's (1868) histogen terminology for describing the mature embryonic root apex of Papaver nudicaule. Each histogen, the plerome, periblem, and dermatogen, presumably represents a group of initials for the three primary embryonic meristems.

The plerome gives rise to the procambium which will differentiate into the primary vascular tissue of the new sporophyte. Procambial cells form a continuous cylinder in the embryo extending into the cotyledons

(Fig. 41,50). At maturity, procambial cells are elongate, densely cytoplasmic containing large nuclei, and occasionally contain small protein bodies (Fig. 47). The periblem gives rise to the cortical ground meristem. Cells of the ground meristem region are characterized at maturity by their vacuolate appearance accompanied by stores of carbohydrates and proteins (Fig. 46,47). The dermatogen gives rise to the root cap as well as the protoderm which eventually forms the epidermis. Cells of the uniseriate protoderm are densely cytoplasmic and at maturity are packed with protein and carbohydrate stores (Fig. 46,47). Cells of the root cap also contain protein and carbohydrate in a dense cytoplasmic matrix (Fig. 46, 48). Possession of a separate morphological histogen for the cortex and a common histogen for the protoderm and root cap corresponds to the type of root apex organization found most frequently in dicotyledons (Popham, 1966). In Papaver nudicaule, histological characteristics of the three primary meristems and their derivatives are in accord with observations of angiosperm embryos in general (Cutter, 1971; Steeves and Sussex, 1972; Esau, 1977).

As the tissues of the embryo differentiate, degeneration of the suspensor takes place resulting in the complete detachment of the embryo just before the embryo reaches maturity (Fig. 46). Suspensors may serve as a source of growth regulators for the developing embryo proper, especially in plants which have elaborate suspensors such as Phaseolus coccineus (Alpi et al., 1975; Cionini et al., 1976; Lorenzi et al., 1978). The notion that the suspensor of Phaseolus produces substances needed by the embryo during development is substantiated by developmental and ultrastructural features (Yeung and Clutter, 1979). To suggest that the suspensor of Papaver nudicaule has a similar function remains speculation.

Endosperm development

Endosperm development in Papaver nudicaule conforms to the nuclear type in which a series of free nuclear divisions of the primary endosperm nucleus is followed by cellularization (Maheshwari, 1950). The primary endosperm nucleus resides in the chalazal portion of the central cell where, soon after fertilization, endosperm nuclei and associated cytoplasm first accumulate as a result of subsequent free nuclear divisions (Fig. 16). Continued synchronous free nuclear divisions result in coenocytic endosperm that resides in the periphery of the central cell about the time a two-celled proembryo has been established (Fig. 18,20). Nuclear endosperm development is initially in the chalaza and continues toward the micropyle as in other members of the Papaveraceae such as Argemone mexicana (Sachar, 1955) and Dendromecon rigida (Berg, 1967). Eschscholzia californica is an exception due to the position of the primary endosperm nucleus near the micropyle and free nuclear endosperm development toward the chalaza along the periphery of the central cell (Sachar and Ram, 1958; Negi, 1974). Stages of the free nuclear mitotic process in Papaver nudicaule were observed in at least two ovules each containing a two-celled proembryo. A cell plate forms in association with the spindle apparatus during late anaphase and persists at least until after the two new sister nuclei are formed (Fig. 19). There is no evidence that a complete wall is formed. The possibility that cell plates formed during free nuclear endosperm divisions represent a mitotic residue (phragmoplast) that eventually breaks down has been suggested (Coulter and Chamberlain, 1912; Schürhoff, 1926). Free nuclear endosperm cell plates may result in walls that initially

compartmentalize endosperm nuclei into groups before major cellularization takes place. Buell (1952a) reported that in Dianthus chinensis free nuclear endosperm, the first cell walls are established by cell plates associated with telophase spindles dividing the free nuclei into groups of three or four prior to wall formation without mitotic spindles. The fate of Papaver nudicaule free nuclear endosperm cell plates remains unclear.

Endosperm cellularization in P. nudicaule starts at the micropyle about the time a filamentous proembryo is established and progresses along the periphery of the central cell toward the chalaza. This directional pattern of cellularization is common in the Papaveraceae (Sachar, 1955; Sachar and Ram, 1958; Berg, 1967). Cellularization is accomplished by the formation of freely growing cell walls arising from the central cell wall in a wavy or crooked pattern (Fig. 25). The cellularization of P. nudicaule endosperm appears similar to cellularization processes described in Helianthus annuus (Newcomb, 1973b), Stellaria media (Newcomb and Fowke, 1973), Triticum aestivum (Morrison and O'Brien, 1976), and Haemanthus katherinae (Newcomb, 1978). Unlike Triticum endosperm (Morrison and O'Brien, 1976), fluorescence microscopy failed to indicate a callose-like component to the developing walls of P. nudicaule endosperm when treated with aniline blue. Subsequent cellularization is accomplished by mitoses accompanied by cell plate formation until the entire central cell is filled with cellular endosperm similar to Haemanthus katherinae (Newcomb, 1978).

Early cellular endosperm of Papaver nudicaule is highly vacuolate, has large nuclei and thin PAS positive staining walls (Fig. 28). The

cytoplasm adjacent to the nuclei contains starch and a few smaller protein bodies. Staining with Sudan black B indicates the beginning of lipid accumulation throughout the cytoplasmic matrix. There appears to be a gradient of maturation resulting in more mature endosperm nearest the embryo and progressively less mature endosperm toward the chalaza. Maturation involves the formation of large protein bodies within the vacuoles, increased lipid content, and an increase in wall thickness (Fig. 29,30). Mature endosperm is, therefore, characterized by large nuclei, the lack of vacuoles, and numerous large protein bodies in a cytoplasmic matrix composed largely of lipid (Fig. 36). Endosperm in members of the Papaveraceae is known to contain a high percentage of both lipid and protein bodies (Röder, 1958; Bewley and Black, 1978). Sachar and Ram (1958) reported that starch grains were a common component of Eschscholzia californica endosperm, but a survey of endosperm throughout the Papaveraceae including Eschscholzia by Röder (1958) and more recently by Berg (1967) indicates that starch is not present. Endosperm protoplasts of Papaver nudicaule are also devoid of carbohydrate stores, but the thick PAS positive staining walls probably provide an accessible carbohydrate source. Endosperm hemicellulosic wall material has been reported to serve as reserve carbohydrate material for embryos of Phytelephas macrocarpa, Phoenix dactylifera, and Coffea arabica (Raghavan, 1976; Bewley and Black, 1978).

Endosperm degradation

Endosperm breakdown presumably provides the needed materials for further growth and development of the embryo (Raghavan, 1976). Degradation begins in the endosperm immediately adjacent to the apex of the early

globular embryo as evidenced by the deterioration of the endosperm cell wall and subsequent protoplast disorganization (Fig. 31,32). Degradation continues to spread involving the endosperm adjacent to and surrounding the entire embryo (Fig. 33). At the time globular embryo protodermal crenulations appear, there is a network of empty cells characterized by their loose arrangement of wall material and conspicuous absence of protoplasts (Fig. 34,35). Continued growth and elongation of the embryo toward the chalaza is preceded by a gradient of endosperm degradation with the embryo as the focus. Deterioration begins with the cell walls which appear to thicken presumably representing a loosening of the wall material (Fig. 37). Continued wall loosening reveals a middle lamellar region between adjacent cells and the eventual exposure of large fibrils extending from both sides of the middle lamellar region (Fig. 38). Fibril appearance begins in the corners and continues to spread along the entire length of the thickened wall (Fig. 38). At the embryo-endosperm interface, the endosperm wall has been reduced to a network of loosely arranged fibrillar material (Fig. 35,38). Once a certain degree of wall loosening has occurred, the lipid filled cytoplasmic matrix appears to undergo digestion leaving the large protein bodies. The lipid is presumably used as a high energy source for further development (Bewley and Black, 1978) and the protein bodies may either be utilized immediately or are broken down and translocated into the developing cotyledons as stores of structural proteins, concentrations of preformed enzymes, or both (Matile, 1976).

The embryo has been implicated as the source of digestive enzymes leading to endosperm breakdown during germination of Lactuca sativa L. seeds (Ikuma and Thimann, 1963). A structural study of endosperm

breakdown in Lactuca sativa revealed that degradation starts within each cell at the plasmalemma and works outward affecting the walls first. This observation and the fact that each cell is equipped for protein synthesis led Jones (1974) to propose that breakdown resulted from endosperm enzyme activity using either preformed enzymes or those synthesized de novo. Halmer et al. (1975) have demonstrated that Lactuca sativa endosperm wall polysaccharide contains a large percentage of mannan as compared with a very low mannan content in embryo walls. Evidence that mannanases are involved in the breakdown of endosperm walls to supply needed polysaccharides to the developing embryo comes from localized mannanase activity within the endosperm of L. sativa during germination (Halmer et al., 1975). The endosperm is presumably the source for the mannanases, although some low level mannanase activity was detected in the embryo which may implicate the embryo as the origin of the enzyme or may represent contamination (Halmer et al., 1976). In Papaver nudicaule, there is morphological evidence for a gradient of endosperm degradation with the embryo as the focal point. This observation in addition to the apparent initiation of breakdown beginning at the embryo-endosperm interface suggests the embryo as the origin of a factor or factors which initiates cell wall loosening and subsequent degeneration. The protodermal crenulations that appear at the late globular stage and persist at the tips of the cotyledons throughout development may also indicate an embryonic influence. The wall crenulations may reflect a wall modification that increases the secretory and/or absorptive surface area. Masand and Kapil (1966) reported that other workers have felt that embryo protoderm especially in cotyledons, is

involved in endosperm digestion, but the exact relationship has not been determined.

Synergids

Shortly after fertilization, the remains of the degenerate synergid appear dense and darkly stained at the time the persistent synergid begins to show signs of degradation (Fig. 12). The large chalazal vacuole of the persistent synergid collapses causing the chalazal boundary of the synergid to become convoluted (Fig. 13). The large nucleus degenerates as the outer perimeter of the filiform apparatus becomes amorphous in appearance and stains more intensely with PAS (Fig. 13,14). Earlier reports of post-fertilization events in the Papaveraceae suggested that both synergids break down before the onset of embryogenesis (Sachar, 1955; Sachar and Ram, 1958). In Dendromecon rigida, however, Berg (1967) stated that the persistent synergid degenerated slowly throughout the early stages of endosperm formation. The persistent synergid in Eschscholzia californica is reported to begin to degenerate a few hours after fertilization as evidenced by the disruption of the tonoplast, nucleus, and the general deterioration of the cytoplasm (Negi, 1974). A portion of the degenerating persistent synergid in Papaver nudicaule exists during early embryogenesis (Fig. 18,27), but is no longer visible during the early globular embryo stage when the cellular endosperm becomes mature.

In some genera the persistent synergid remains intact presumably to nourish the embryo in cases where endosperm formation is retarded (Maheshwari, 1948). In genera such as Ammobium and Cotula the persistent synergids may enlarge or eventually form haustoria to facilitate

translocation of nutrients into the post-fertilization megagametophyte (Davis, 1961, 1962). The persistent synergid in Helianthus annuus was found to degenerate very slowly and maintain ultrastructural features necessary for a high metabolic and synthetic capability. These observations led Newcomb (1973b) to suggest that the persistent synergid may be involved in the translocation of metabolites to the developing embryo and endosperm. The morphological evidence in Papaver nudicaule and other members of the Papaveraceae indicate that the persistent synergid after fertilization is no longer metabolically active and, therefore, unlikely to play any major role in the nutrition of the developing seed. It is possible, however, that metabolites and breakdown materials from the degradation of persistent synergid are utilized during embryo and/or endosperm development.

Antipodals

Following fertilization and during free nuclear divisions of the endosperm, the three antipodals continue to enlarge within the megagametophyte. Antipodals continue to be characterized by a polarity expressed by large micropylar vacuoles, large chalazal nuclei, but chalazal wall ingrowths are more extensive (Fig. 15). These large cells persist throughout the very early stages of Papaver nudicaule embryogenesis (Fig. 21). Shaw (1904) observed that in the Papaveraceae the antipodals of Eschscholzia, Sanguinaria, and Chelidonium persisted during various stages of endosperm formation. A survey of antipodal morphology in the Papaverales conducted by Huss (1906) revealed other genera such as Corydalis, Fumaria, Dicentra, and Papaver also have large antipodals which persist up to certain stages of seed development. These early reports

led Schürhoff (1926) to conclude that antipodal enlargement and persistence are characteristic for the Papaveraceae, a conclusion supported by more recent studies (Sachar, 1955; Sachar and Ram, 1958; Berg, 1967; Negi, 1974). In Argemone mexicana, the antipodals enlarge and maintain their morphology up to the time a heart-shaped embryo has been established (Sachar, 1955). Sachar and Ram (1958) reported that the antipodals of Eschscholzia californica enlarged and after fertilization, remained intact until cellularization of the endosperm. In post-fertilization ovules of Dendromecon rigida, the antipodals proliferate until their number reaches approximately 30-50 cells all of which persist until cellular endosperm has filled the central cell (Berg, 1967). More recently, the post-fertilization antipodals of Eschscholzia californica were shown to retain ultrastructural features associated with metabolically active cells such as high concentrations of mitochondria and numerous dictyosomes until their degeneration which coincides with endosperm cellularization (Negi, 1974). Negi (1974) also observed presumed dictyosome vesicles coalescing with numerous smaller vacuoles to form the large micropylar vacuole. During antipodal breakdown, the thin micropylar wall ruptures releasing the vacuolar contents into the central cell. These observations led Negi (1974) to suggest that antipodal vacuolar contents contribute to the initiation and development of endosperm cell walls. In Papaver nudicaule, degeneration of the antipodals also occurs about the time endosperm cellularization takes place and is accompanied by breakdown of the chalazal wall ingrowths, deterioration of the large nuclei, and the loss of the micropylar vacuole presumably as a result of micropylar wall breakdown giving the cells an overall

flattened appearance (Fig. 24). About the time a globular octet embryo has formed, the antipodals have completely disappeared.

Nucellus

The post-fertilization micropylar nucellus of Papaver nudicaule remains unchanged retaining large nuclei, vacuolate cytoplasm, and starch, except for remnants of the pollen tube (Fig. 12,13). This pad of nucellus remains intact until the embryo proper begins to differentiate from the proembryo. The nucellar cytoplasm becomes disorganized as the cells are compressed which results in the eventual break down of the micropylar nucellus as the embryo becomes globular. A persistent nucellar pad was reported in other genera of the Papaveraceae such as Argemone and Eschscholzia (Sachar, 1955; Sachar and Ram, 1958), but the situation in Papaver nudicaule is again similar to Dendromecon in that the micropylar nucellus is eventually destroyed (Berg, 1967).

The peripheral nucellus consists of a single layer of large, highly vacuolate cells containing starch. These cells also undergo cytoplasmic disorganization and wall compression as the cellularization of the endosperm takes place (Fig. 25). About the time the endosperm is completely cellular, the peripheral nucellus appears disorganized (Fig. 28). The expanded central cell eventually replaces the peripheral nucellus (Fig. 29). Observations in Papaver nudicaule conflict with the report by Berg (1967) that the persistence of a layer of peripheral nucellus until the seed reaches maturity is characteristic in the Papaveraceae.

The nucellus in the post-fertilization chalaza remains segregated into a region of degrading cells and a region of intact cells. The nucellus in the area of the hypostase continues to show a gradient of

degradation with breakdown more pronounced near the antipodals. Cytoplasm of the crushed cells at the antipodal-nucellus interface stains intensely for protein and exhibits substantial concentrations of starch (Fig. 15). The remaining cells within the degenerating zone appear enlarged and show various stages of cytoplasmic deterioration (Fig. 16). Post-fertilization expansion of the central cell continues during early endosperm development resulting in the gradual encroachment upon the degenerating chalazal nucellus and hypostase (Fig. 22). The deterioration of hypostase cells involves the disorganization of the protoplast followed by an increase in PAS positive staining material within the lumina presumably as a result of wall breakdown. During endosperm cellularization and antipodal deterioration, the expanding central cell replaces the degenerated nucellus and forms an interface with the region of intact nucellar cells, destroying the hypostase in the process (Fig. 24). During the later stages of seed maturation, the intact nucellus eventually becomes restricted to a small region in the chalaza near the funiculus.

Seed coat

Inner integument -- The first indication that post-fertilization changes in the integuments of Papaver nudicaule are underway is the appearance of an osmiophilic material that stains lightly with PAS in the vacuoles of the inner epidermis (Fig. 25,28). Accumulation of osmiophilic substances begins in the cells nearest the micropyle and gradually spreads toward the chalaza, continuing until the cell lumina are filled (Fig. 29). Similar osmiophilic substances have been observed in cells of developing tendril adhesive discs (Endress and Thomson, 1976) and

in the early differentiation of cotton ovule fibers where the substance also stained positively with PAS (Ramsey and Berlin, 1976). On the basis of histochemical testing, the authors of both reports suggested that the osmiophilic material is composed primarily of phenolic compounds. Upon P. nudicaule seed coat maturation, the inner epidermis consists of empty lumina and thick radial walls that eventually become undulated from compression (Fig. 40,49). Corner (1976) refers to these cells as "tracheidal" because some of the phenolic substances are incorporated into the cell walls and may influence water permeability and germination (Werker et al., 1979). Protoplasts of the mesophyll layer disintegrate resulting in empty, thin walled cells. This layer collapses and is often difficult to identify in contrast to the cells of the outer epidermis that elongate as wall thickening occurs. In the mature seed coat this layer is comprised of longitudinal fibers (Fig. 40,49).

Outer integument -- The cells of the inner epidermis become compressed resulting in the condensation of the cytoplasm (Fig. 28,29). About the time of cotyledon initiation, protoplast disruption occurs and the thin walled cells are crushed as the seed coat matures (Fig. 40,49). The protoplasts of the large cells of the outer epidermis also deteriorate as the outer tangential walls thicken and become concave (Fig. 49). This layer of cells comprises the main mechanical layer which classifies the Papaver seed coat as exotestal (Corner, 1976).

Post-fertilization changes in both integuments of Papaver nudicaule are similar to those reported earlier for other members of the genus Papaver (Meunier, 1891; Röder, 1958). Although structural differences

exist between genera, seed coat characteristics of P. nudicaule are typical for the Papaveraceae (Corner, 1976).

Development without placental attachment

Internal ovular development in Papaver nudicaule is arrested when fertilized ovules are removed from their placentae at 4 and 6 days after in vitro pollination and sown on fresh medium. In 4 day old seeds, both endosperm cellularization and embryo differentiation cease. In 6 day old seeds, further development fails even though the endosperm is cellular and there is a small globular embryo. In contrast, seeds removed from their placentae 8, 15, and 22 days after pollination in vitro continue to develop internally with most seeds reaching maturity. The presence of mature endosperm appears to be the single most important morphological criterion for continuation of internal development in ovules detached from their placentae. Eight days after pollination, seeds contain globular embryos and exhibit the first morphological evidence for mature endosperm degradation (Fig. 31). These results from P. nudicaule do not agree with reports of in vitro seed development to maturity in ovules of P. somniferum detached from their placentae and containing either zygotes or two-celled proembryos (Maheshwari, 1958). Subsequent studies by Maheshwari and Lal (1961) indicated that even though early stages of the post-fertilization ovule could be cultured to maturity on a nutrient medium without exogenous hormones and without placental attachment, development in vitro appeared slower than in vivo. Maheshwari and Lal (1961) decided to test the effects various additives to the medium would have on embryos from cultured ovules without placentae.

Casein hydrolysate added to the medium promoted both embryo growth and differentiation. Yeast extract added to the medium promoted embryo differentiation, but embryos were small. The addition of certain cytokinins to the medium was reported to promote embryo differentiation, but inhibit embryo elongation. Gibberellic acid disrupted the elongation and differentiation of cotyledons only, in contrast to the overall inhibition of embryo development when the medium was supplemented with auxin. Pontovich and Sveshnikova (1966) repeated the earlier Papaver somniferum experiments of Maheshwari (1958), but were unable to obtain continued development in ovules removed from placentae at either the zygote or two-celled proembryo stage. The data from P. nudicaule substantiate the conclusion of Pontovich and Sveshnikova (1966) that the early stages of post-fertilization ovule development in vitro are dependent on the placenta.

Post-fertilization Ovule In Vivo

Early seed development -- Ovules examined 4 days after hand pollination in vivo reveal a two-celled proembryo in the micropylar end of the megagametophyte (Fig. 51). The apical cell is smaller than the basal cell, although the nuclei appear to be the same size. The cytoplasm of each cell is vacuolate and contains starch. The large central cell vacuole restricts the free nuclear endosperm to the periphery. The three large chalazal antipodals feature highly developed chalazal wall ingrowths and large nuclei (Fig. 52). The micropylar nucellus is composed of small cells that contain starch in dense cytoplasm in contrast to the larger, more vacuolate peripheral nucellus.

The nucellus in the chalazal end of the ovule reveals a region of intact nucellus and a region of nucellar degradation including a hypostase. Numerous PAS positive carbohydrate containing bodies accumulate in the vacuolate zone of nucellar breakdown at the nucellus-megagametophyte interface near the antipodal chalazal wall ingrowths (Fig. 52). Carbohydrate accumulation near the antipodals may be required for endosperm cellularization. Osmiophilic substances also begin to accumulate in the tonoplast periphery of the inner epidermis of the inner integument at this stage (Fig. 51). Morphological changes in the integuments are initiated near the micropyle, but eventually spread along the entire length of the integuments toward the chalaza.

Examination of seeds 9 to 10 days following hand pollination in vivo reveal a small globular embryo accompanied by a multicellular suspensor embedded in mature cellular endosperm (Fig. 53). The cells of the embryo proper stain more intensely than the suspensor and the cytoplasm of both structures contains starch. The enlarged central cell is now completely filled with cellular endosperm accompanied by the destruction of the antipodals. Endosperm cells have PAS positive staining walls, lipid filled cytoplasm, numerous large protein bodies, and large nuclei. During this stage of seed development, a symmetrical pattern of endosperm degradation with the embryo at the center occurs. Most of the nucellus has been crushed by the expanding central cell. Seed coat differentiation is also well underway in both integuments.

Twelve days after in vivo pollination, major changes in internal seed morphology can be seen in the embryo. The cells of the incipient protoderm are as dense but contain more starch than the cells comprising the subdermal tissue of the embryo proper (Fig. 54). The outer tangential

walls of the incipient protoderm are crenulated and form an inter-digitation with the network of adjacent endosperm cell walls. The mitotic derivatives of the hypophysis are now distinct and possess staining characteristics similar to the suspensor. The multicellular suspensor stains less intensely than the embryo proper and also contains starch.

Embryo elongation and the differentiation of the three primary meristems and their derivatives becomes apparent after two weeks of ovular development in vivo (Fig. 55). Procambium will differentiate from the densely cytoplasmic, elongated, innermost cells of the embryo that contain very little starch. The larger cells of the cortical ground meristem that surrounds the presumptive procambial core contain numerous starch granules. The outer tangential walls of the uniseriate presumptive protoderm remain crenulated and the densely cytoplasmic cells also possess numerous starch granules.

Endosperm degradation continues as embryo growth and differentiation proceed. The gradient of degradation illustrates the pattern followed by individual endosperm cells as they are broken down (Fig. 56). The relatively thin PAS positive staining walls appear to thicken which may actually represent a loosening of the wall material. Further loosening of the wall material reveals a middle lamellar region and the eventual appearance of large fibrils that extend from the middle lamellar regions between endosperm cells. The final stages of wall loosening start in the corners and spread along the entire length of the wall resulting in a network of fibrillar material. Deterioration of the lipid filled cytoplasm begins at various times during the wall

loosening process. Endosperm cells lose their cytoplasmic matrix first followed by the eventual breakdown of the large protein bodies.

Mature seed structure -- Internal examination of seeds collected from mature capsules reveals a complete embryo. Organization of the epicotyl dome is characterized by a random arrangement of large cells that contain large nuclei, but stain less intensely than the neighboring tissue (Fig. 57). These embryonic apical cells fit the morphological criteria attributed to "initials" (Fahn, 1974; Esau, 1977). There is no clear differentiation between an incipient tunica and corpus as defined by Schmidt (1924). The embryonic root apex, in contrast, is organized into three distinct tiers (Fig. 58). The component cells of each tier appear to stain less intensely than surrounding tissue and have large nuclei. Each tier is also associated with one of the three primary meristems and their derivatives. According to Hanstein (1868), each tier represents one of three histogens, the plerome, the periblem, and the dermatogen. The plerome gives rise to the procambium region, the periblem gives rise to the cortical ground meristem, and the dermatogen gives rise to both the protoderm and the root cap.

Incipient procambial cells are elongated parallel with the direction of embryo elongation and have dense cytoplasm. The cortical ground meristem and its derivatives have large nuclei and a cytoplasm less dense than the procambium. Cells of the cortical ground tissue are filled with carbohydrates, proteins, and lipids. The cells of the uniseriate protoderm are also filled with carbohydrates, proteins, and lipids, but stain more intensely than the cortical ground tissue. The root cap is poorly developed consisting of only one layer of intensely staining cells. Cotyledon anatomy reflects the same tissue composition

as the main embryonic axis and differentiation of procambium presumably is acropetal as in other genera (Steeves and Sussex, 1972).

The embryo is embedded in several layers of endosperm. An extended region of endosperm chalazal to the cotyledons shows the various stages of degradation. The outermost layer of the seed coat has thick walled cells with concave outer tangential walls. This layer corresponds to the main mechanical layer of the Papaver seed coat (Corner, 1976). The mechanical layer is subtended by a region of crushed cells. The next intact layer of the seed coat is composed of longitudinal fibers orientated parallel with the longitudinal axis of the embryo. The fibers are also subtended by a region of crushed cells. The innermost layer of the seed coat is comprised of compressed cells with thick radial walls. The general morphology of the albuminous seeds of Papaver nudicaule is characteristic of the family (Corner, 1976).

Discussion

The nutritional aspects of Papaver nudicaule embryogenesis may be considered in three phases. The first phase is concerned with embryo nutrition prior to the onset of endosperm degradation, the second phase with the embryo-endosperm interaction, and the third phase with embryo nutrition at the time of germination through seedling establishment. Evidence supporting phase interrelationships is based on morphology and limited histochemistry.

The central cell and its contents provide the environment in which the zygote will develop into an embryo. As was previously discussed, the central cell probably serves as a nutrient reservoir. The central

cells of some angiosperms develop transfer cell-like wall ingrowths that remain intact beyond fertilization and into the early stages of embryogenesis. In Pisum sativum, numerous wall projections are distributed inside the post-fertilization megagametophyte along the periphery, but more elaborate projections form in the chalazal region near the developing embryo (Marinos, 1970). Wall ingrowths in Helianthus annuus megagametophytes persist in the micropylar region near the egg apparatus after fertilization (Newcomb and Steeves, 1971). Wall projections are eventually covered over by developing endosperm walls, but not until embryogenesis is underway. This observation indicates that the central cell may be active in the direct translocation of metabolites into the megagametophyte during early seed development (Newcomb and Steeves, 1971; Newcomb, 1973b). Negi (1974) observed wall ingrowth formation in the micropylar region of the central cell of Eschscholzia californica and suggested the possibility of a more efficient metabolite translocation into the megagametophyte during early embryogenesis as a result of the wall projections. Even though the post-fertilization central cell of Papaver nudicaule does not develop wall ingrowths, it is possible that the entire surface of the central cell wall is capable of metabolite absorption (Newcomb, 1973b).

Previous studies suggested the integuments and nucellus as the most likely sources for the metabolites that accumulate in the post-fertilization megagametophyte (Marinos, 1970; Newcomb and Steeves, 1971; Newcomb, 1973b; Negi, 1974). In Papaver nudicaule, the nucellus contains numerous starch granules and begins to degenerate as the megagametophyte reaches maturity. Following fertilization, the central cell continues to expand until maximum megagametophyte size is reached which is

approximately when the globular embryo appears and the endosperm is mature. During the process of post-fertilization expansion, the megagametophyte replaces all of the nucellus except the region of intact nucellus in the chalaza.

Prior to destruction of the hypostase during megagametophyte expansion, the region of nucellar degradation in the chalaza is filled with starch in the vicinity of the antipodal chalazal wall ingrowths. A single vascular strand terminates in the chalazal nucellus near the hypostase which is in close proximity to the base of the antipodals. The antipodals of P. nudicaule maintain transfer cell morphology throughout the early stages of seed development. Antipodal persistence and structural association with the hypostase suggests their involvement in the translocation of metabolites into the megagametophyte during early embryogenesis.

The second phase of embryo nutrition centers on the interaction between embryo and endosperm. Endosperm is considered to be a primary nutrient storage tissue that is digested and utilized by the developing embryo (Maheshwari, 1950; Masand and Kapil, 1966; Raghavan, 1976). Morphological evidence supporting the nutritive role of endosperm can be summarized in two general observations. First, the proximal relationship between the localized breakdown of intact endosperm and the growth and differentiation of the embryo is construed as evidence for the digestion and utilization of endosperm by the embryo (List and Steward, 1965; Raghavan, 1976; Bewley and Black, 1978). Second, in specialized cases where endosperm does not develop, such as in the Orchidaceae, the embryo may develop haustoria-like structures that presumably draw

nourishment from other ovarian tissues as a substitute for endosperm (Masand and Kapil, 1966; Raghavan, 1976).

In Papaver nudicaule, endosperm cells feature PAS positive staining walls, large protein bodies in a lipid filled cytoplasmic matrix, and large nuclei. Endosperm breakdown appears to begin in the cells adjacent to the young globular embryo and as the embryo grows the pattern of endosperm degradation expands as well. During the later stages of embryogenesis, the region of endosperm chalazal to and in the path of embryo elongation breaks down. As a result, an elongate, fully differentiated embryo occupies the central region of the seed previously occupied by endosperm. The observations of the developmental and structural relationship between the embryo and endosperm in Papaver nudicaule implicate partial, if not total, embryo dependence on endosperm food reserves.

The suspensors of some angiosperm embryos have been implicated in embryo nutrition. In Capsella bursa-pastoris (Schulz and Jensen, 1968b; Schulz and Jensen, 1969) and Stellaria media (Newcomb and Fowke, 1974), the suspensor basal cell develops wall ingrowths during the early stages of embryogenesis and probably functions as a transfer cell (Gunning and Pate, 1969; Pate and Gunning, 1972). As embryogenesis continues, other cells of the suspensor also develop wall ingrowths, presumably to facilitate metabolite translocation into the embryo proper from the endosperm until a heart-shaped embryo has formed (Schulz and Jensen, 1969). In Papaver nudicaule, the suspensor contains carbohydrates and proteins during the early stages of embryo development and shows signs of deterioration only after cotyledon initiation. The basal cell maintains a large vacuole from the two-celled proembryo stage up to and including the stage

when the incipient protoderm of the globular embryo becomes crenulated. It is possible that the suspensor cells, especially the basal, may function nutritionally during early embryogenesis of P. nudicaule and may continue in this capacity until the transition to endosperm breakdown is complete.

The third phase of embryo nutrition involves the transition from a germinating, heterotrophic embryo to the establishment of an autotrophic seedling. In exalbuminous dicotyledonous seeds, most food reserves are located in the cotyledons of the embryo. In contrast, albuminous dicotyledonous seeds provide endosperm in addition to the cotyledons as a food reserve for the embryo during germination. There is reserve food mobilization and translocation into the embryonic axis in either case (Raghavan, 1976). During mobilization, the concentrations of insoluble sugars, polysaccharides, soluble nitrogen, proteins and RNAs decrease in the cotyledons and increase in the embryonic axis (Raghavan, 1976; Bewley and Black, 1978). Sze and Ashton (1971) suggested that hormones originating in the embryonic axis are responsible for regulation of enzymes involved in mobilization from the cotyledons to the axis in Cucurbita maxima. More recent studies by Davies and Chapman (1979a,b) showed that during food mobilization in Cucumis sativus the embryonic axis removes the breakdown products of proteins and lipids from the cotyledons. Davies and Chapman (1979a,b) hypothesized that enzymes for food mobilization are inhibited by high concentrations of food degradation end products and, therefore, the embryonic axis promotes mobilization by keeping end product concentrations low. At the present time, there is no experimental evidence permitting speculation on the execution of the last phase of embryo nutrition in Papaver nudicaule.

Ovule attachment to the placenta is required during the early stages of seed development in Papaver nudicaule. The placenta may provide morphogenetic factors to the post-fertilization ovule, influence metabolite translocation into the ovule, or both (Raghavan, 1976). Buell (1952b) reported the starch content in the placental tissues of Dianthus chinensis to be at a maximum at the time of fertilization. The placental and funicular starch reserves were depleted during the early stages of embryogenesis as the starch content in the ovular tissues increased. Buell (1952b) concluded that the placenta probably provides a reserve source of metabolites required for early development. The starch filled placentae of P. nudicaule begin to show signs of deterioration in vitro about the time endosperm becomes mature (Olson, unpublished). One possible interpretation of this observation is that the P. nudicaule placentae serve as a metabolite source and/or accumulate additional metabolites from the growth medium for subsequent translocation into the ovule. The possibility that placentae also produce morphogenetic factors that may be required for differentiation of the early embryo and/or endosperm maturation should not be ruled out.

The stage in Papaver nudicaule at which ovular attachment to the placenta is not necessary for continued development coincides with the completion of endosperm maturation. During this period of growth, the globular embryo is associated with endosperm degradation as tissue regions of the embryo proper begin to differentiate. Sachar and Kapoor (1959) studied embryogenesis in Zephyranthes ovules and recognized two major phases. The first phase is characterized by a series of mitotic divisions to produce the mass of cells of the globular embryo. This

process appears to be independent of endosperm because embryo cell numbers continue to increase when endosperm development is arrested. The second phase is characterized by differentiation of the cell mass. The presence of endosperm is essential if normal differentiation is to occur. Sachar and Kapoor (1959) suggested the endosperm as the source of morphogenetic factors influencing embryo differentiation. Morphogenetic factors in the endosperm may be endogenous seed hormones (Raghavan, 1976). Auxins have been detected in the endosperm of a variety of angiosperms such as Pyrus malus (Luckwill, 1948, 1953) and Cassia fistula (Mukherjee et al., 1966). The highest levels of auxin in the fruit of C. fistula occur midway between fertilization and fruit ripening and high auxin levels are correlated with endosperm cellularization. These observations lead Mukherjee et al. (1966) to conclude that the endosperm is the auxin source in C. fistula. Gibberellin-like substances have also been isolated from the endosperms of Echinocytis, Lupinus, Phaseolus, and Pharbitis (Corcoran and Phinney, 1962; Ogawa, 1963a,b). The mature endosperm of Papaver nudicaule appears to have an essential role in embryo differentiation implicating the endosperm as a source of growth regulators.

Three days after pollination in vitro, a two-celled proembryo is established in the micropylar region of the P. nudicaule megagametophyte. This stage of embryogenesis is accompanied by free nuclear endosperm and three large antipodals in the chalazal end of the megagametophyte. These morphological features obtained in vitro are virtually identical to the internal morphology of ovules obtained four days after hand pollination in vivo (compare Fig. 18,21 with 51,52). The establishment of a young

globular embryo and mature endosperm 8 to 9 days post-pollination in vitro is soon followed by endosperm degradation (Fig. 31-33). A similar internal morphology is demonstrable in ovules developed in vivo 9-10 days after hand pollination (Fig. 53). Crenulation of the incipient protoderm of globular embryos occurs 10 days post-pollination in vitro and between 11 and 12 days after hand pollination in vivo. A similar sequence of morphological changes in the endosperm during degradation occurs in vitro and in vivo and in both cases the embryo appears to be the focus of the degradation process. It seems reasonable to conclude that seed developmental morphology in vitro does not differ significantly from seed developmental morphology in vivo. The major difference between the two systems appears to be one of timing. Developmental stages are achieved 1-2 days earlier in vitro than in vivo. Kanta and Maheshwari (1963) reported that fertilization and the subsequent stages of seed development in Papaver somniferum also occurs 1-2 days earlier in vitro compared with in vivo. Fertilization presumably takes place earlier in vitro because of the elimination of the rest of the gynoecial tissue. Pollen tubes originating from pollen in direct contact with the ovules, would not have to travel the distance of the stigma and style and would, therefore, take less time.

The later stages of Papaver nudicaule embryogenesis in vitro demonstrate a greater degree of differentiation and growth than that observed in vivo. The organization of the embryonic shoot apex in seeds produced in vitro 27 days after placental pollination illustrates an immature tunica-corpus arrangement (Fig. 47). In contrast, the organization of the embryonic shoot apex in seeds produced in vivo reflects a random arrangement (Fig. 57). The embryonic root apex in 27 day old

seeds produced in vitro clearly demonstrates morphological histogens and a well developed root cap consisting of several layers (Fig. 46,48). Although the embryonic root apex in seeds developed in vivo also reveal histogen organization, the root cap consists only of a single layer of cells and is poorly defined (Fig. 58). The seeds of P. nudicaule produced in vitro appear to contain larger, more differentiated embryos than do seeds produced in vivo. Kanta et al. (1962) and Kanta and Maheshwari (1963) noted an enhancement of overall development during the later stages of embryogenesis in seeds of P. somniferum produced in vitro compared to seeds produced in vivo. One possible explanation for the apparent difference between the in vitro and in vivo systems is the higher concentration and availability of nutrients in vitro. The ovules would conceivably be the only nutrient "sink" and would not have to compete with other sporophytic tissues. It may also be that there is a higher moisture availability in vitro that would inhibit normal seed desiccation and, therefore, enable embryo development to reach its full potential.

The apparent difference in the degree of growth and differentiation between seeds formed in vitro and in vivo may have implications for the definition of a "mature" seed. Does "mature" imply that the seed is germinable, that internal development is complete, or both? Functionally mature seeds are capable of germination under natural environmental conditions. Morphologically mature seeds achieve their full potential for internal structural development. Stokes (1952) reported that when "mature" seeds of Heracleum sphondylium become dormant, the embryo is undifferentiated. In order to germinate the seeds must be imbibed and kept at low temperatures for several months. Endosperm food reserves

are mobilized at low temperatures (2-5C) and the embryos of H. sphondylium continue development until they are fully differentiated prior to germination. In "mature" seeds of plants such as Anemone nemorosa, Caltha palustris, Ficaria verna, Fraxinus nigra, and F. excelsior, the embryos are differentiated, but are not as fully developed as they are just before germination. These seeds are not morphologically mature when they are shed, but after imbibition and under favorable temperatures, the embryos complete their development (Villiers and Wareing, 1964; Raghavan, 1976; Wareing and Philips, 1978). Seeds of Papaver nudicaule developed in vitro achieve morphological maturity 27-28 days after placental pollination and are capable of germinating within 1-2 days of reaching this stage (Fig. 50). Seeds produced in vitro from 22 day old cultures are capable of germination 5-8 days beyond their stage of development (Fig. 41). These data suggest that functional maturity may be achieved at a developmental stage not yet morphologically mature. The "mature" seed of P. nudicaule produced in vivo contains an embryo at a similar stage of morphological differentiation as an embryo in a seed from a 22 day old placental culture (compare Fig. 44,45 with 57,58). These observations suggest that in nature, seeds of P. nudicaule only develop as far as necessary to achieve functional maturity prior to dessication and dispersal. If this notion is correct, it is also probable that once a seed is rehydrated, embryo differentiation continues and the embryo becomes morphological mature in preparation for germination.

ABBREVIATIONS USED IN FIGURES AND CAPTIONS

ABB	aniline blue black
An	antipodals
BC	basal cell
C	cotyledon
CC	central cell
CP	cotyledon primordium
D Sy	degenerate synergid
E	embryo
EC	epicotyl
En	endosperm
FA	filiform apparatus
Fn	funiculus
GM	ground meristem region
HC	hypocotyl
Hd	hypophysis derivatives
Hy	hypostase
IC	immature corpus
IT	immature tunica
Nu	nucellus
Ov	ovule
P	protoderm
PAS	periodic acid-Schiff's
PG	pollen grain
Pl	placenta
PP	incipient protoderm
Pr	procambial region
P Sy	persistent synergid
PT	pollen tube
RC	root cap
S-FG	safranin-fast green
SN	secondary nucleus
Su	suspensor
TC	terminal cell
Z	zygote
i	plerome
ii	periblem
iii	dermatogen
1	outer epidermis of outer integument
2	inner epidermis of outer integument
3	outer epidermis of inner integument
4	mesophyll of inner integument
5	inner epidermis of inner integument

Fig. 1: Scanning electron micrograph of pre-pollination ovule. x 178.

Fig. 2: Scanning electron micrograph of ventral surface of pre-pollination, detached ovule. Arrow indicates location of micropyle. x 383.

Fig. 3: Scanning electron micrograph of ovules 15 hrs. post-pollination in vitro. Most pollen tube growth along ovular surface is random. x 200.

Fig. 4: Scanning electron micrograph of germinated pollen grain 6 hrs. post-pollination in vitro. Beaded appearance of pollen tube is due to callose plugs. x 1023.



- Fig. 5: Light micrograph of longitudinal section through pre-fertilization synergids. The section is stained with PAS-ABB. Note massive filiform apparatuses. x 813.
- Fig. 6: Light micrograph of longitudinal section through egg. The section is stained with PAS-ABB. Egg polarity same as synergids. x 1148.
- Fig. 7: Light micrograph of longitudinal section through chalazal end of pre-fertilization ovule. The section is stained with PAS-ABB. Arrows indicate antipodal chalazal wall ingrowths. Arrowheads indicate interface between degenerating and intact nucellus. x 462.
- Fig. 8: Light micrograph of secondary nucleus (SN) situated in chalazal region of central cell adjacent to antipodals. The section is stained with PAS-ABB. x 768.

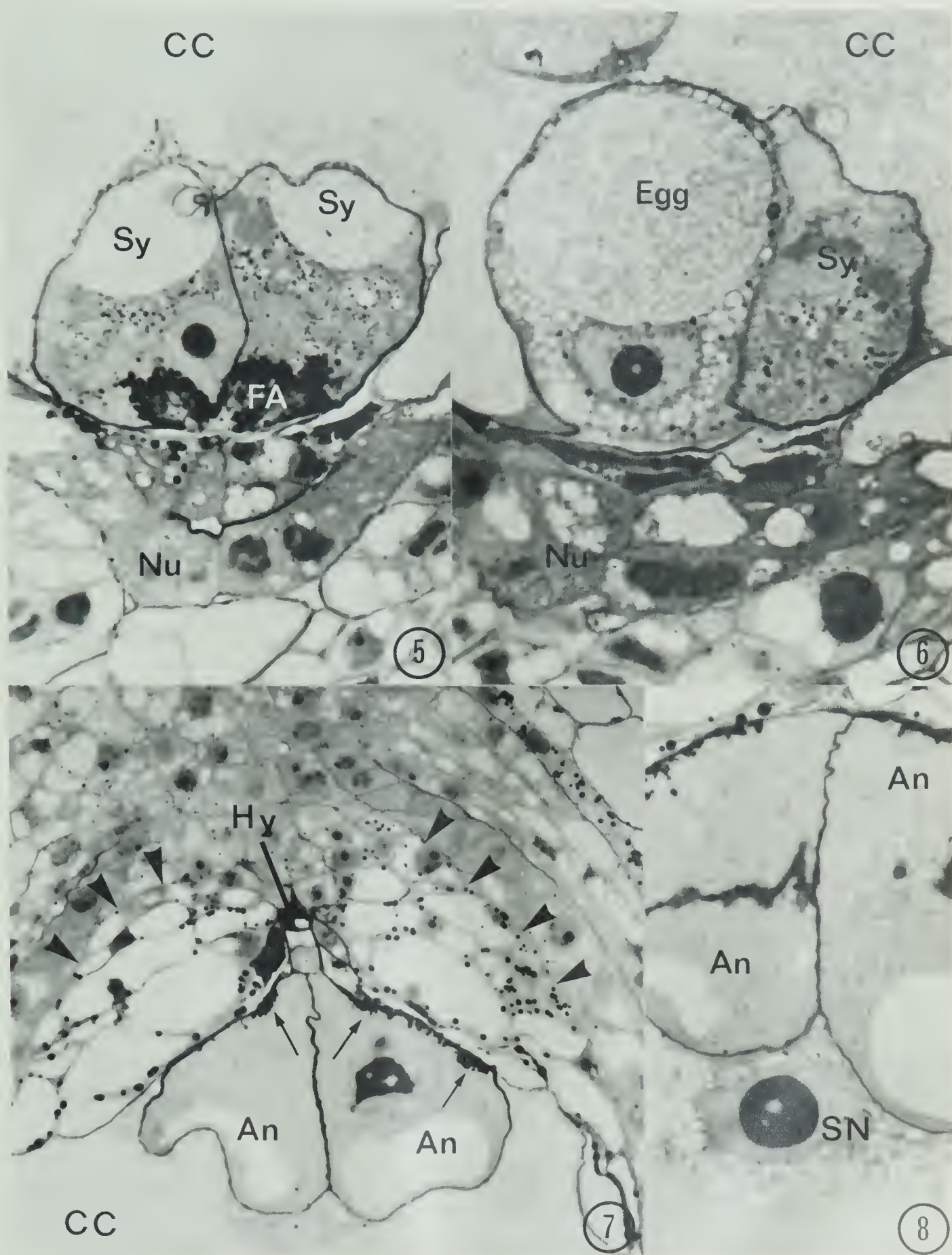
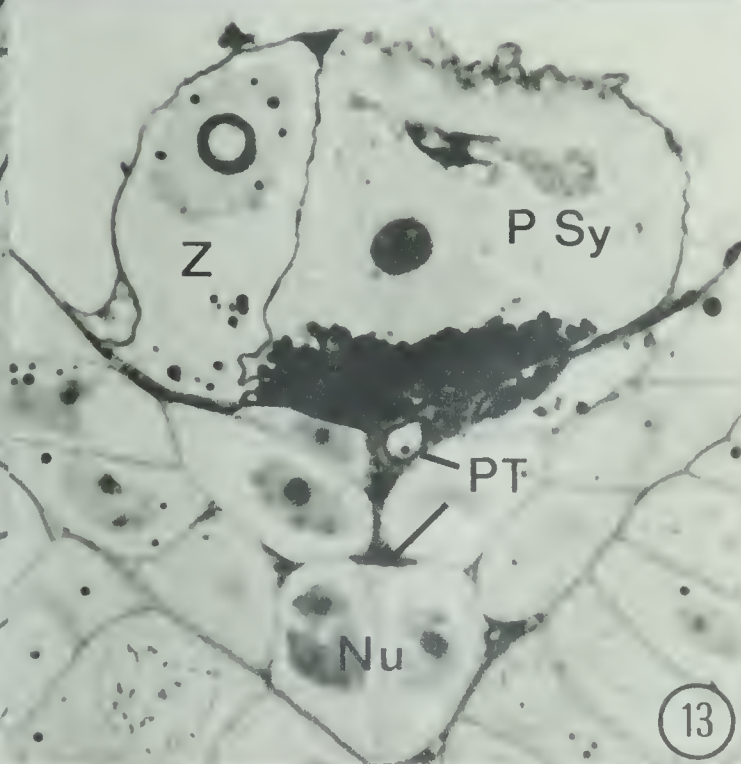
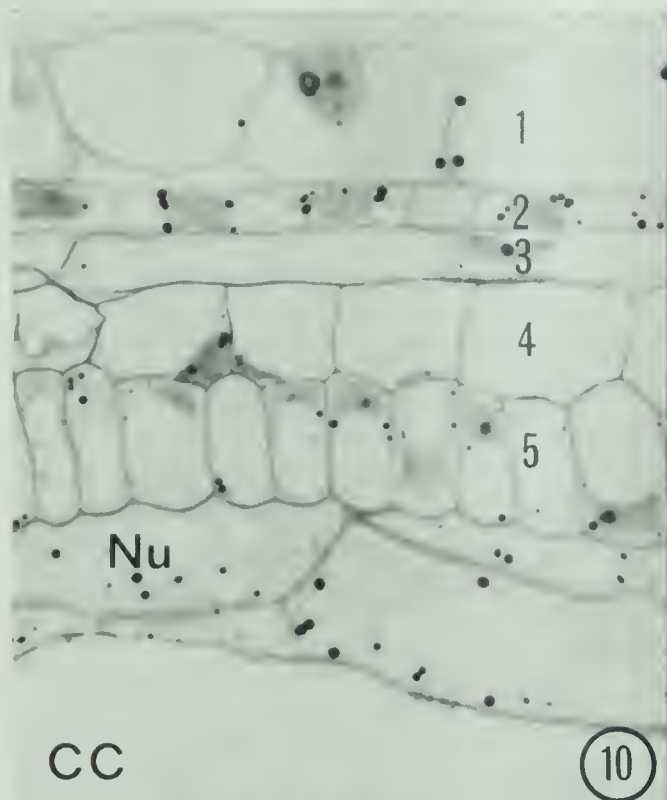


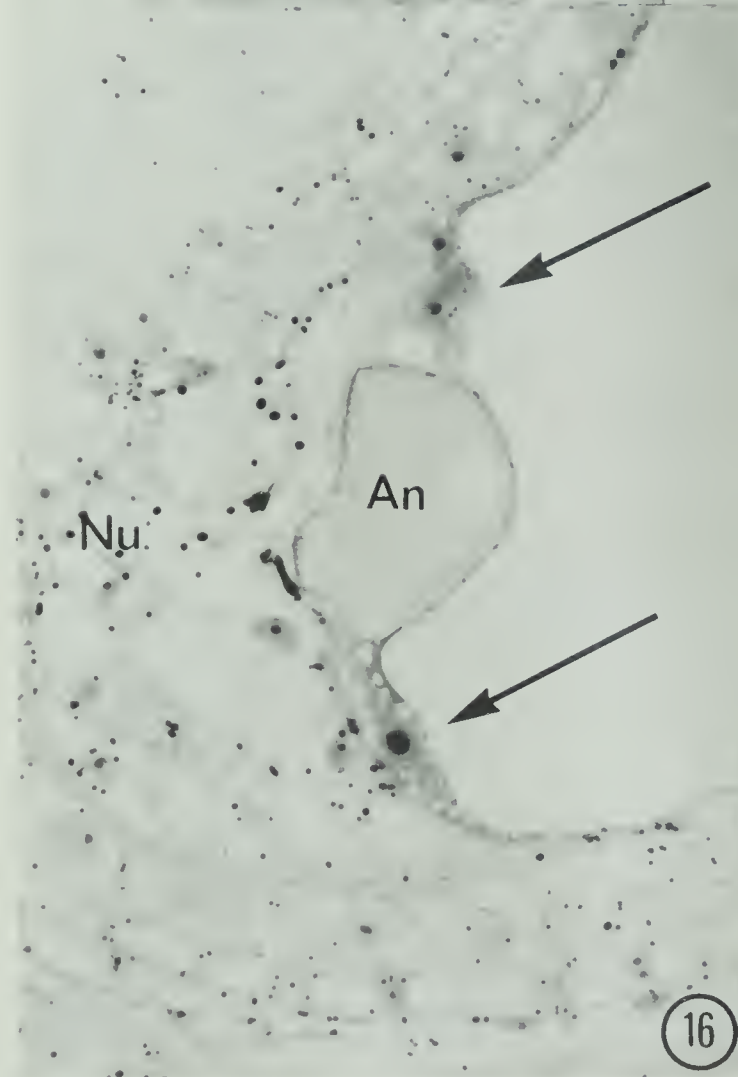
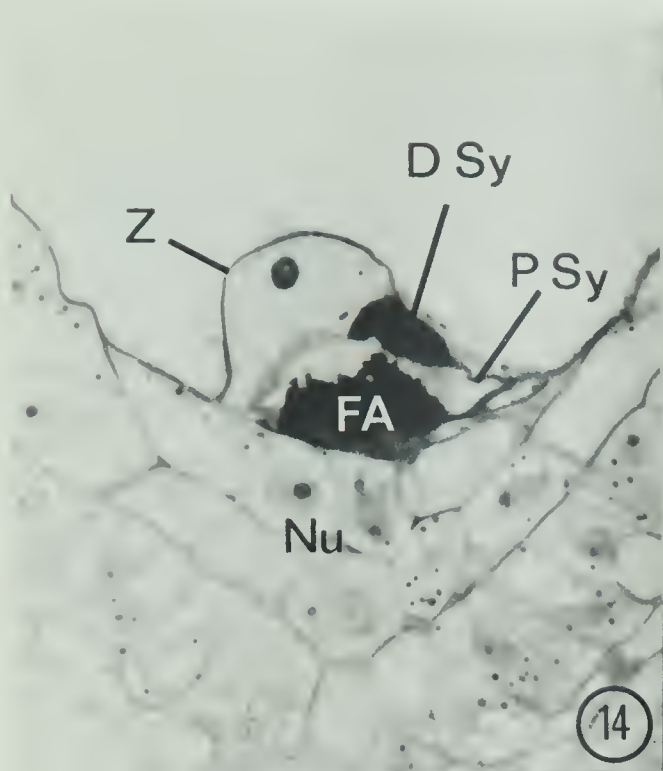
Fig. 9: Scanning electron micrograph of ovule penetrated by pollen
tube 15 hrs. post-pollination in vitro. x 306.



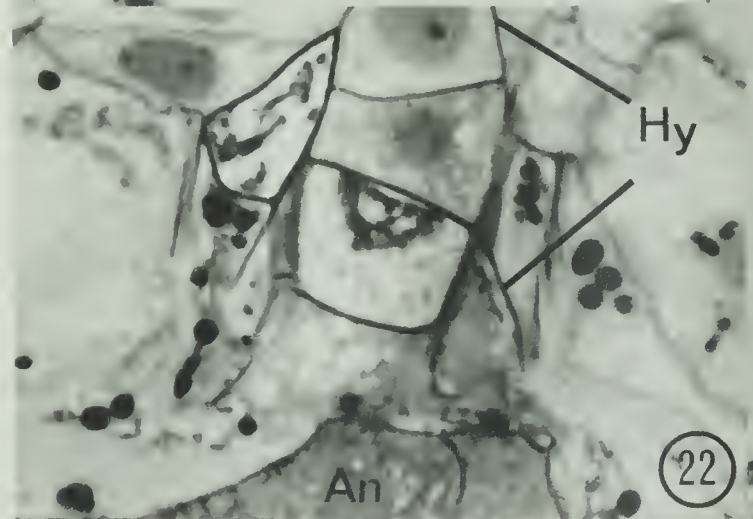
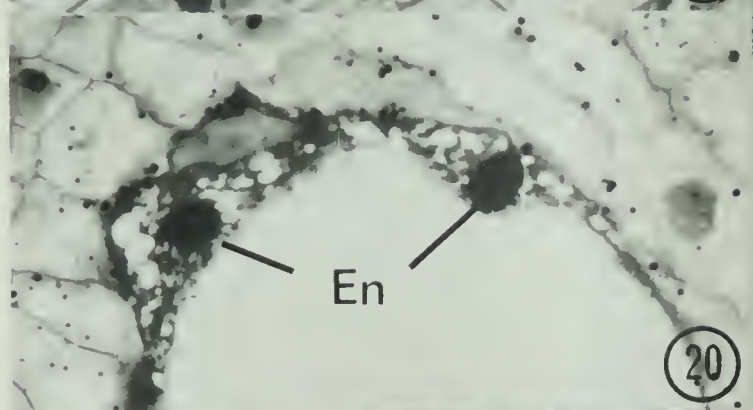
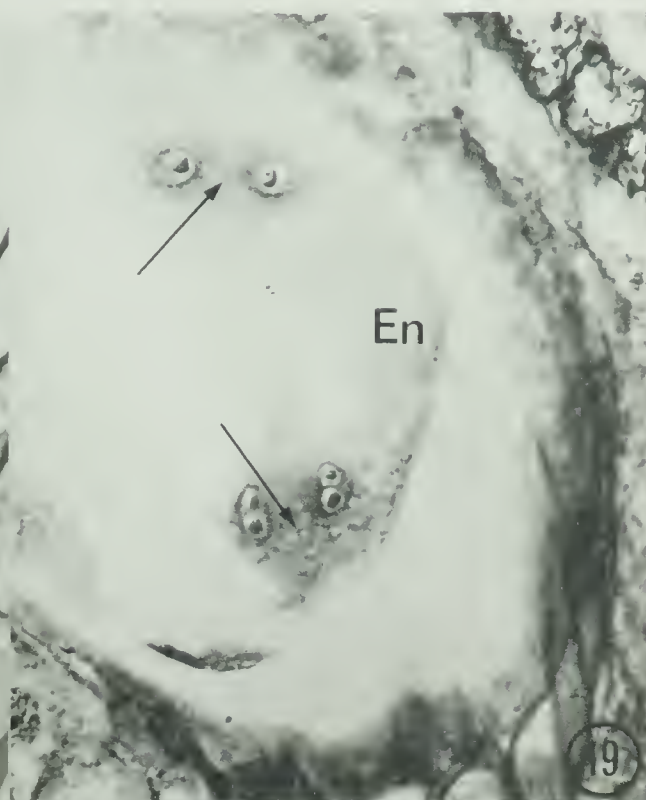
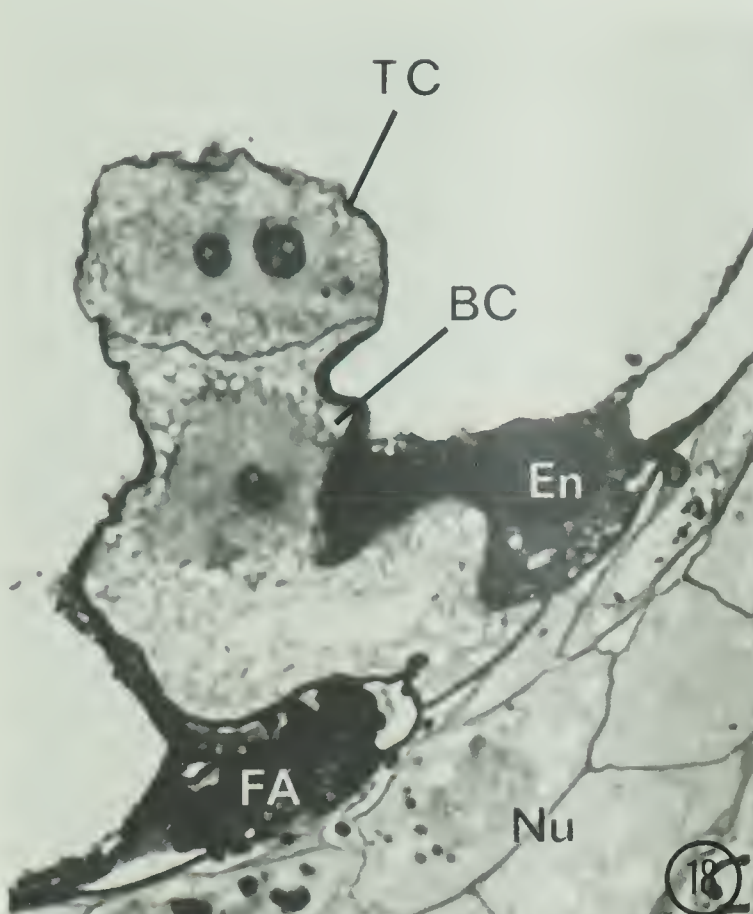
- Fig. 10: Light micrograph of longitudinal section through pre-fertilization integuments and nucellus. The section is stained with PAS-ABB. x 800.
- Fig. 11: Fluorescence micrograph of detached ovule penetrated by pollen tube 24 hrs. post-pollination in vitro. The tissue is treated with aniline blue. Pollen tube fluorescence due to callose-like wall components. x 147.
- Fig. 12: Light micrograph of longitudinal section through degenerate and persistent synergids 26 hrs. post-pollination in vitro. The section is stained with methylene blue. Degenerate synergid penetrated by pollen tube. x 1008.
- Fig. 13: Light micrograph of longitudinal section through early zygote and persistent synergid 2 days post-pollination in vitro. The section is stained with PAS-ABB. Deterioration of persistent synergid underway. x 1116.



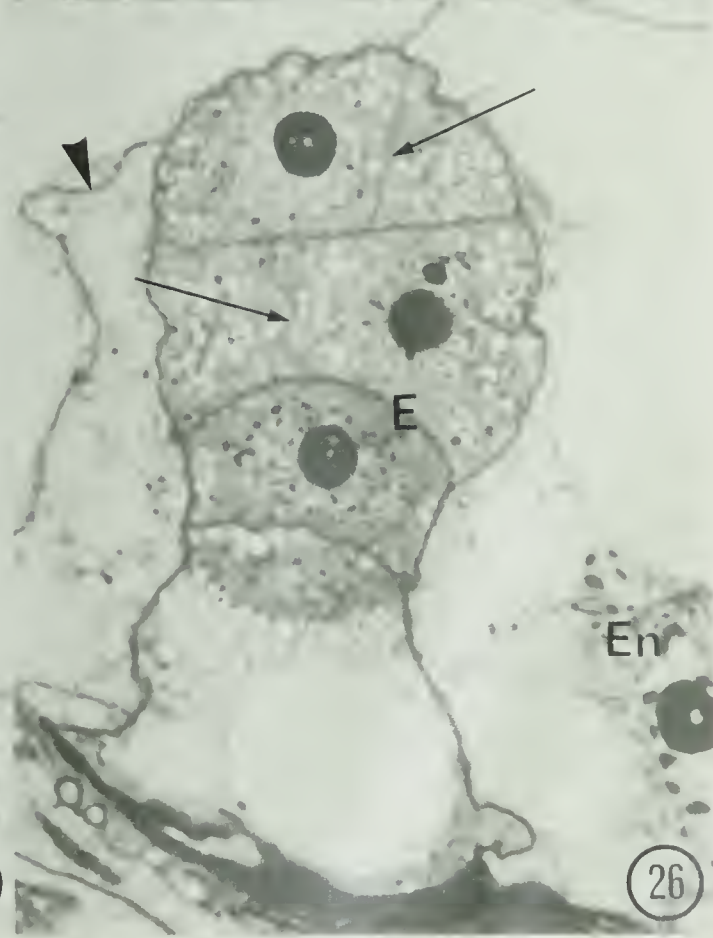
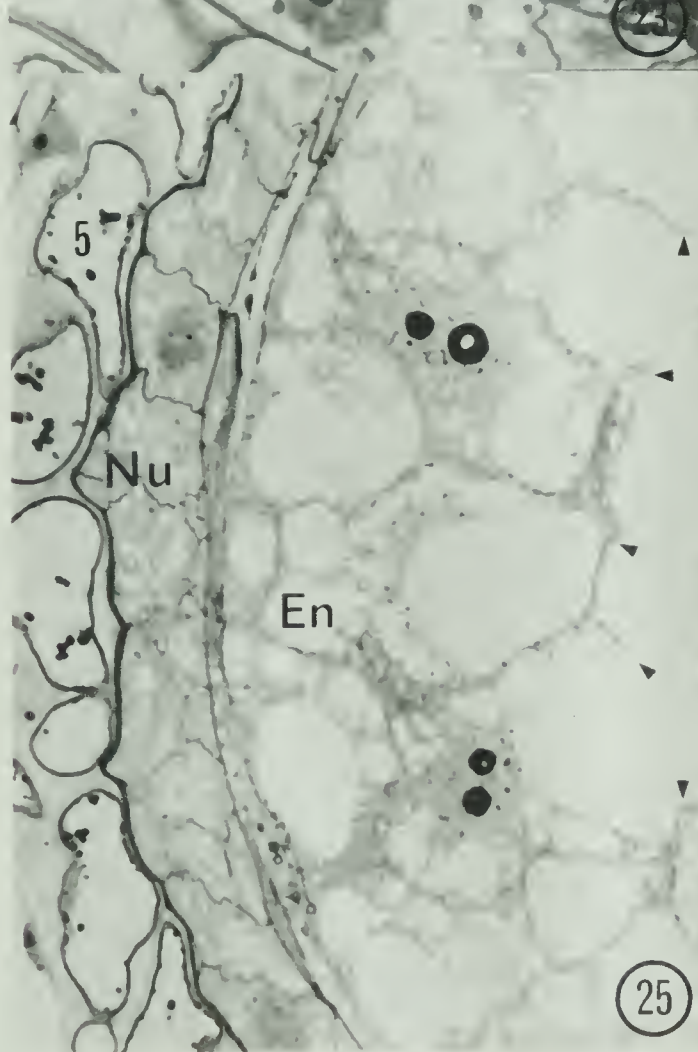
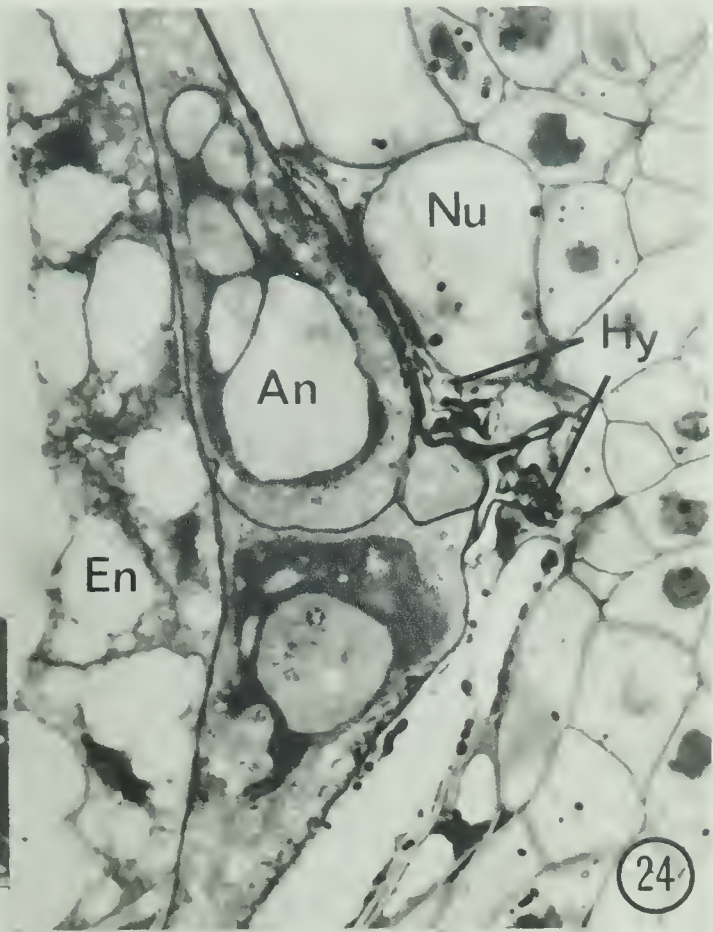
- Fig. 14: Light micrograph of longitudinal section through micropylar region of megagametophyte 2 days post-pollination in vitro. The section is stained with PAS-ABB. Note thick zygote wall. x 576.
- Fig. 15: Light micrograph of longitudinal section through antipodals 2 days post-pollination in vitro. The section is stained with PAS-ABB. Arrows indicate well developed antipodal wall ingrowths. x 655.
- Fig. 16: Light micrograph of longitudinal section through chalazal region of megagametophyte 2 days post-pollination in vitro. The section is stained with PAS-ABB. Arrows indicate first mitotic derivatives of the primary endosperm nucleus. x 375.
- Fig. 17: Light micrograph of longitudinal section through zygote. The section is stained with PAS-ABB. Note large chalazal nucleus. x 1120.



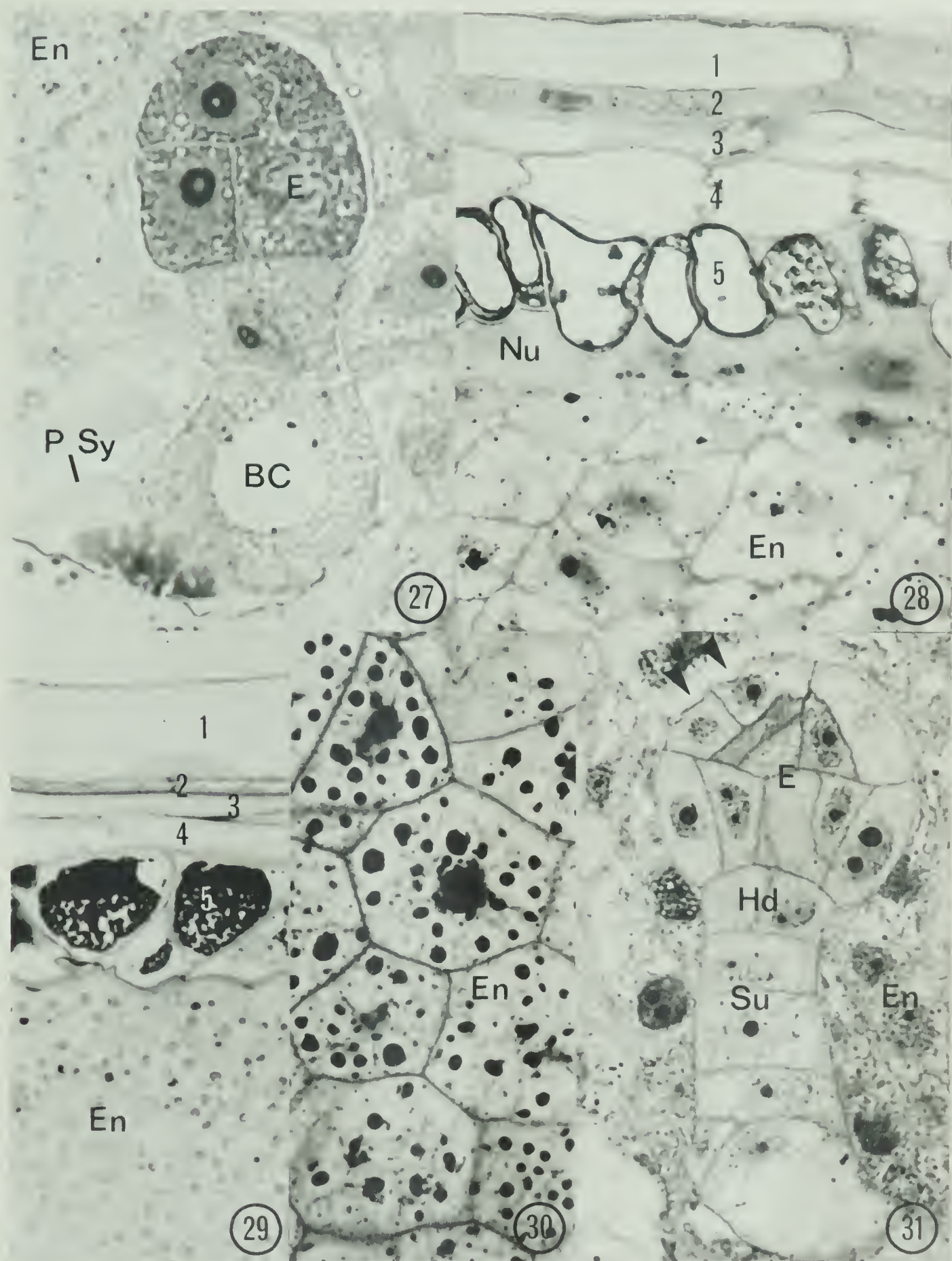
- Fig. 18: Light micrograph of longitudinal section through two-celled proembryo 3 days post-pollination in vitro. The section is stained with methylene blue. x 1302.
- Fig. 19: Nomarski interference micrograph of free nuclear endosperm cell plates (arrows) 3 days post-pollination in vitro. Paraffin embedded section stained with S-FG. x 390.
- Fig. 20: Light micrograph of free nuclear endosperm 3 days post-pollination in vitro. The section is stained with PAS-ABB. x 425.
- Fig. 21: Light micrograph of oblique section through persistent antipodals 3 days post-pollination in vitro. The section is stained with PAS-ABB. x 407.
- Fig. 22: Light micrograph of longitudinal section through thick walled hypostase 3 days post-pollination in vitro. The section is stained with PAS-ABB. x 1451.



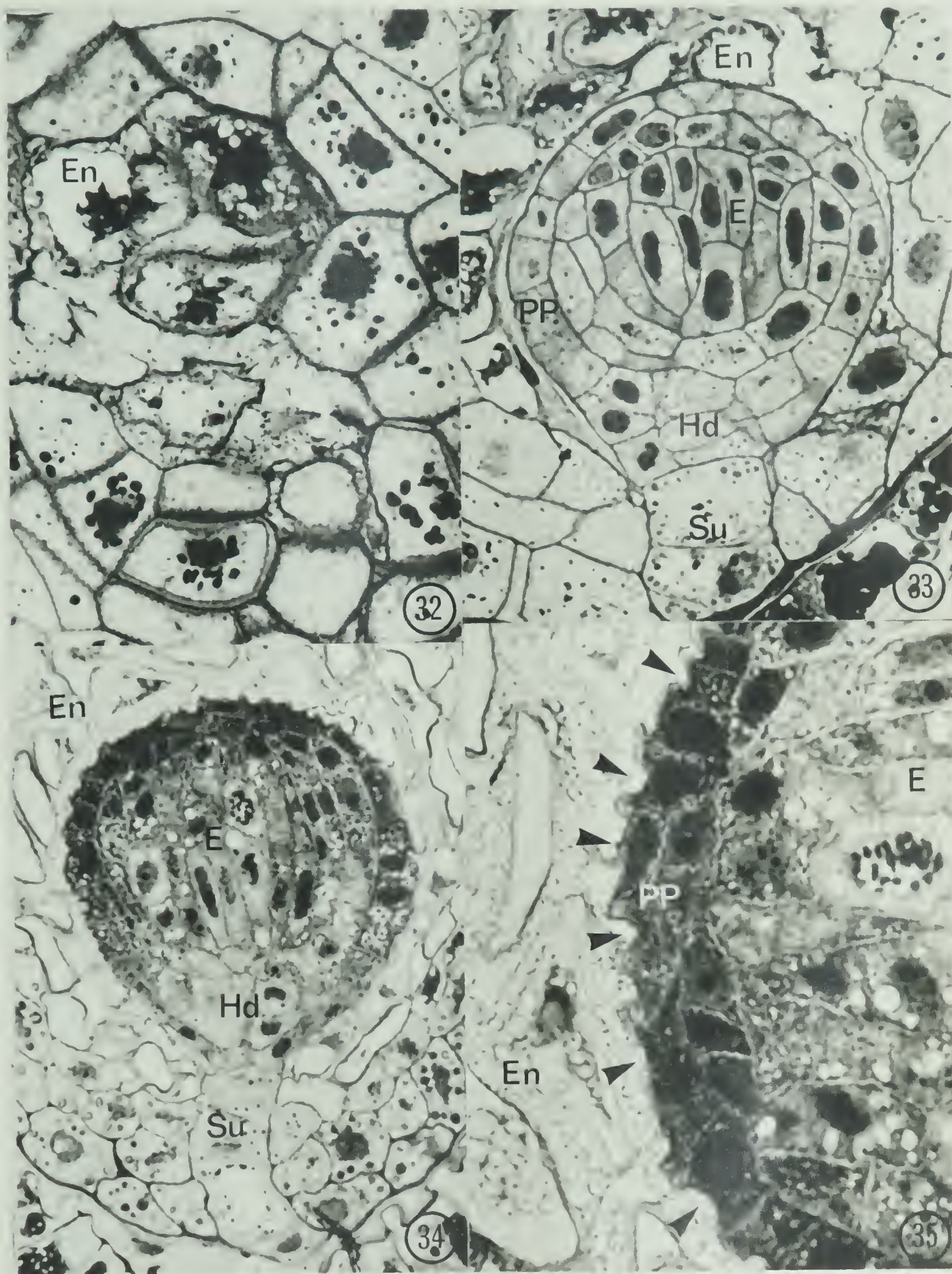
- Fig. 23: Light micrograph of longitudinal section through embryo 4 days post-pollination in vitro. The section is stained with methylene blue. Arrow indicates first vertical cell wall of a filamentous proembryo cell. x 1176.
- Fig. 24: Light micrograph of longitudinal section through antipodals and hypostase 4 days post-pollination in vitro. The section is stained with PAS-ABB. Note deterioration of antipodals and hypostase. x 600.
- Fig. 25: Light micrograph of free nuclear endosperm cellularization 4 days post-pollination in vitro. The section is stained with methylene blue. Arrowheads indicate tip regions of freely growing walls. x 549.
- Fig. 26: Light micrograph of longitudinal section through embryo 4-5 days post-pollination in vitro. The section is stained with methylene blue. Arrows indicate cell walls from first and second vertical divisions of filamentous proembryo cells. Large arrowhead indicates freely growing endosperm cell wall. x 1296.



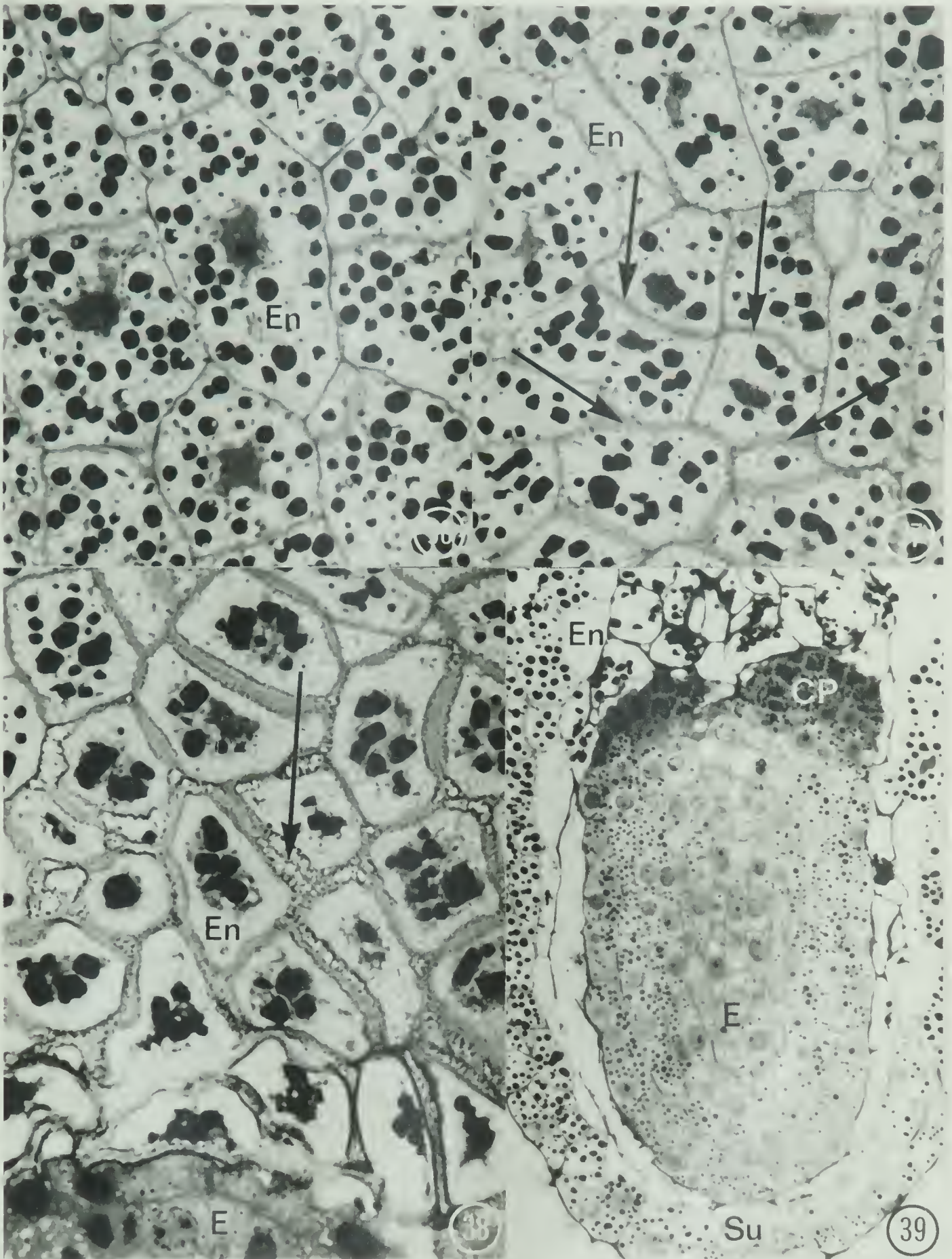
- Fig. 27: Light micrograph of longitudinal section through early globular embryo 6 days post-pollination in vitro. The section is stained with methylene blue. Note large basal cell vacuole. x 1296.
- Fig. 28: Light micrograph of longitudinal section through integuments, nucellus, and endosperm of seed 6 days post-pollination in vitro. The section is stained with PAS-ABB. Endosperm is completely cellular. x 720.
- Fig. 29: Light micrograph of longitudinal section through integuments and endosperm of seed 8 days post-pollination in vitro. The section is stained with methylene blue. Peripheral nucellus is no longer identifiable. Note osmiophilic substance in the inner epidermis of the inner integument (5). x 686.
- Fig. 30: Light micrograph of endosperm from seed 8 days post-pollination in vitro. The section is stained with PAS-ABB. Note developing large protein bodies. x 945.
- Fig. 31: Light micrograph of longitudinal section through globular embryo 8 days post-pollination in vitro. The section is stained with methylene blue. Arrowheads indicate region where endosperm first appears to breakdown. x 882.



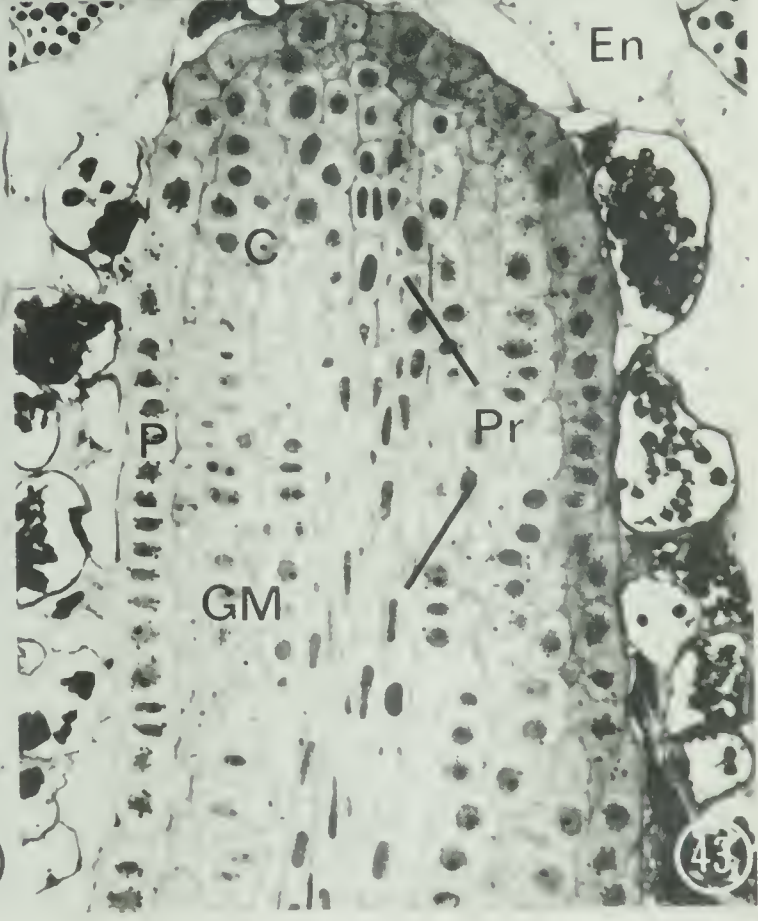
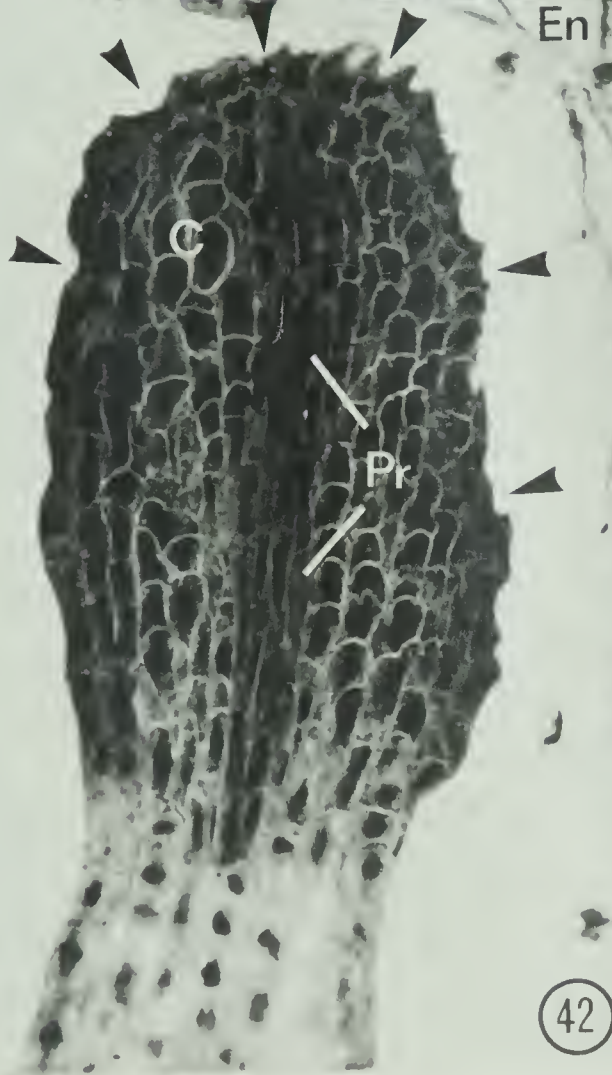
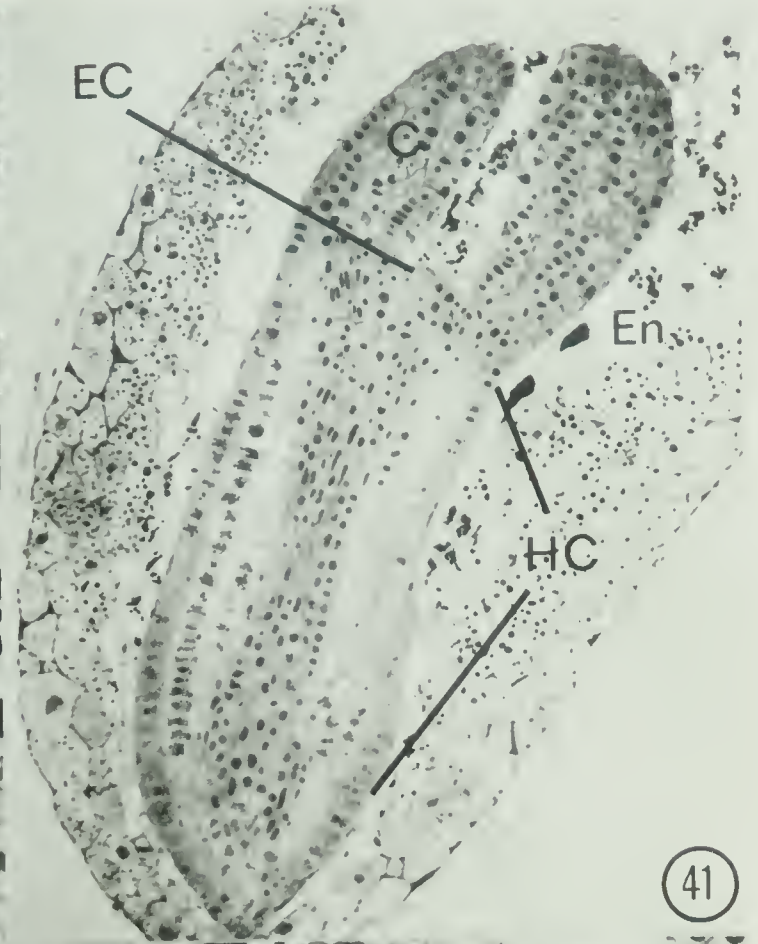
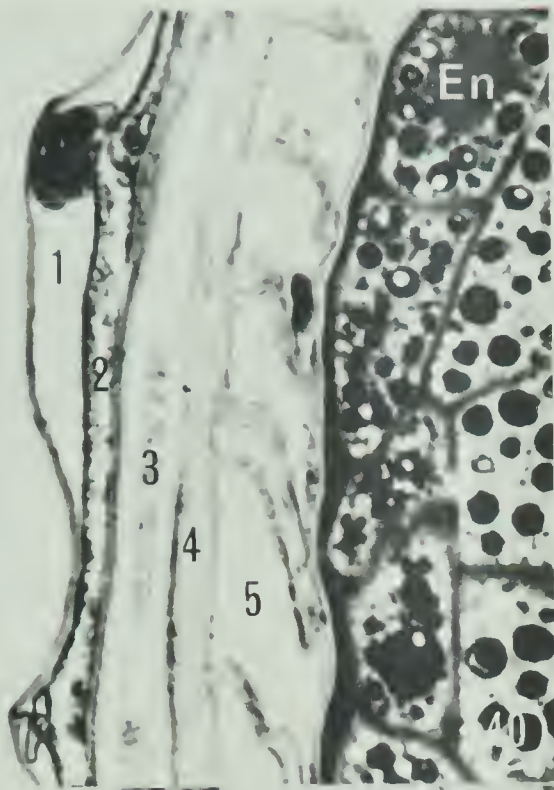
- Fig. 32: Light micrograph of tangential section through endosperm adjacent to globular embryo 8-9 days post-pollination in vitro. The section is stained with PAS-ABB. Endosperm cells nearest embryo show greatest degree of degradation. x 907.
- Fig. 33: Light micrograph of longitudinal section through globular embryo 9 days post-pollination in vitro. The section is stained with methylene blue. Note smooth appearance of outer tangential walls of incipient protoderm (PP). x 697.
- Fig. 34: Light micrograph of longitudinal section through globular embryo 10 days post-pollination in vitro. The section is stained with methylene blue. Note crenulated incipient protoderm. x 587.
- Fig. 35: Light micrograph of embryo-endosperm interface detail 10 days post-pollination in vitro. The section is same as in Fig. 34 and stained with methylene blue. Arrowheads indicate crenulations in outer tangential walls of presumptive protoderm. x 1612.



- Fig. 36: Light micrograph of mature endosperm 10 days post-pollination in vitro. The section is stained with PAS-ABB. Note relatively thin cell walls. x 819.
- Fig. 37: Light micrograph of early stages of endosperm degradation 10 days post-pollination in vitro. The section is stained with PAS-ABB. Arrows indicate initial thickening of endosperm walls presumably as a result of wall material loosening. x 819.
- Fig. 38: Light micrograph of final stages of endosperm degradation 10 days post-pollination in vitro. Arrow indicates site of further wall loosening where fibrils appear on either side of middle lamellar region. x 819.
- Fig. 39: Light micrograph of longitudinal section through embryo 12-13 days post-pollination in vitro. The section is stained with PAS-ABB. Cotyledon initiation occurs at this stage. x 480.



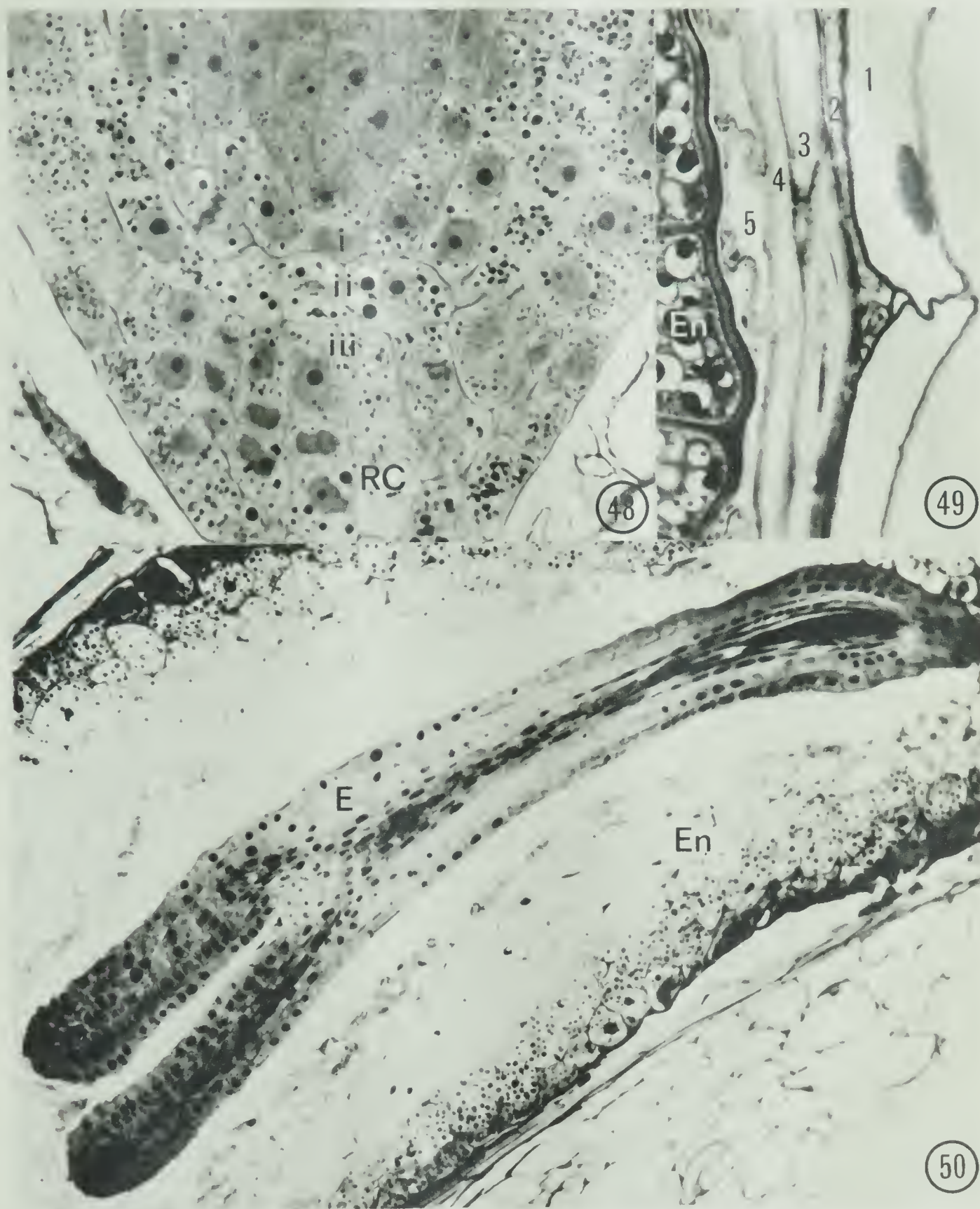
- Fig. 40: Light micrograph of longitudinal section through seed coat 20-22 days post-pollination in vitro. The section is stained with PAS-ABB. Note thickened radial walls of the inner epidermis of the inner integument (5). x 1008.
- Fig. 41: Light micrograph of longitudinal section through entire seed 22 days post-pollination in vitro. The section is stained with PAS-ABB. x 149.
- Fig. 42: Light micrograph of longitudinal section through cotyledon 24-25 days post-pollination in vitro. The section is stained with methylene blue. Arrowheads indicate crenulation in cotyledon protoderm. x 440.
- Fig. 43: Light micrograph of longitudinal section through cotyledon 26 days post-pollination in vitro. The section is stained with PAS-ABB. Note smooth appearance of outer tangential surface of the cotyledon protoderm. x 386.



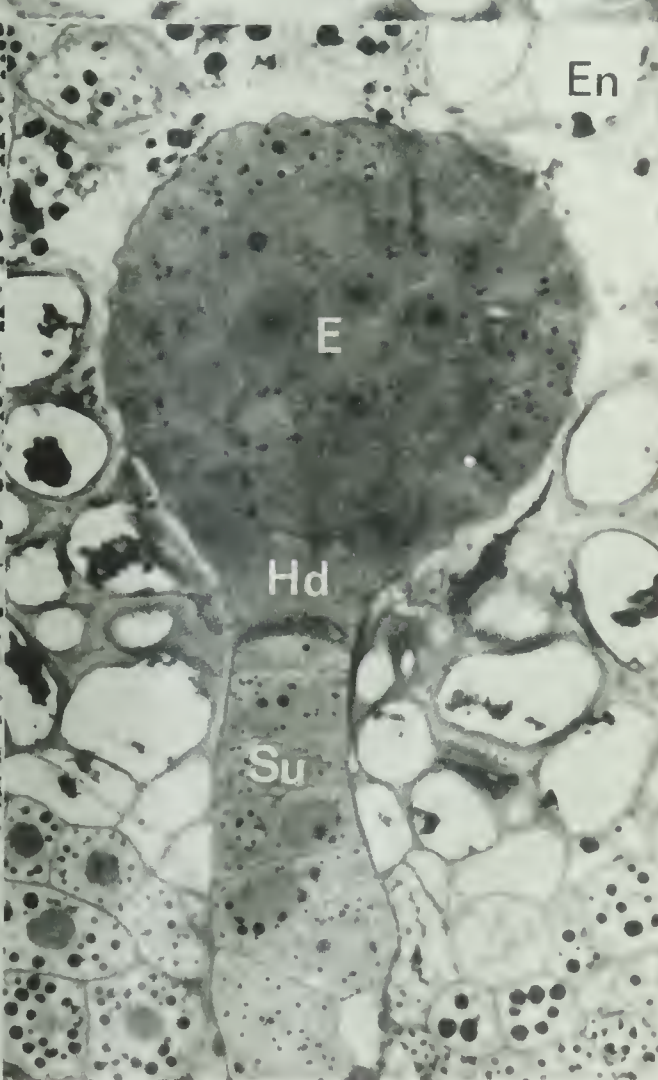
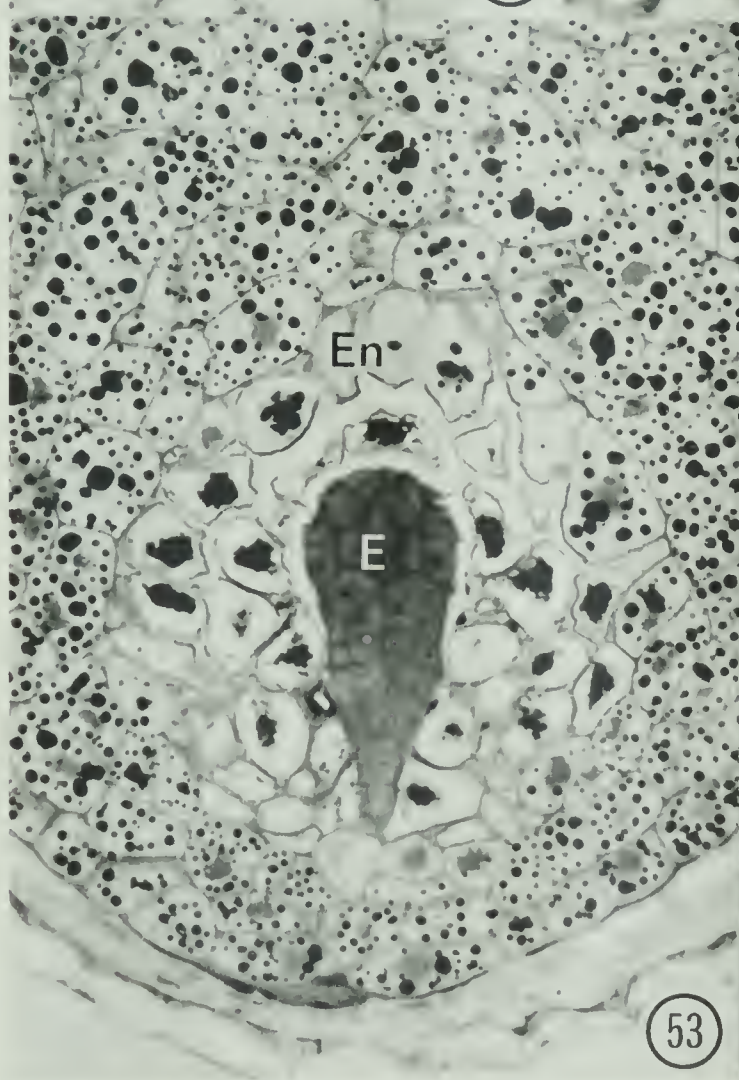
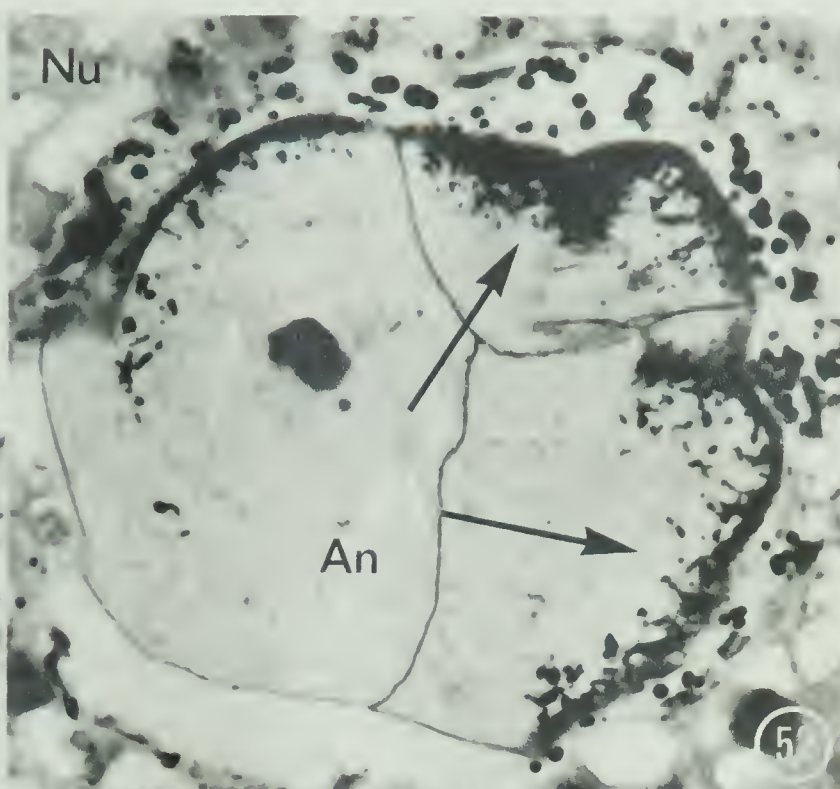
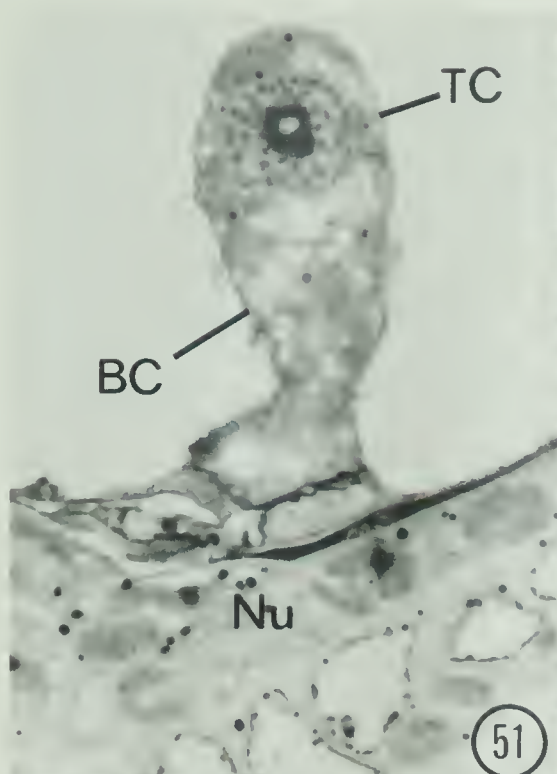
- Fig. 44: Light micrograph of longitudinal section through embryonic shoot apex region 22 days post-pollination in vitro. The section is stained with PAS-ABB. Note random arrangement of epicotyl cells (EC). x 380.
- Fig. 45: Light micrograph of longitudinal section through embryonic root apex region 22 days post-pollination in vitro. The section is stained with PAS-ABB. Tiers of root apex become more distinct. x 380.
- Fig. 46: Light micrograph of longitudinal section through embryonic root apex region in mature seed produced in vitro. The section is stained with PAS-ABB. Suspensor detachment has occurred. x 380.
- Fig. 47: Light micrograph of longitudinal section through embryonic shoot apex region in mature seed produced in vitro. The section is stained with PAS-ABB. Immature tunica-corpus organization of epicotyl can be seen. x 380.



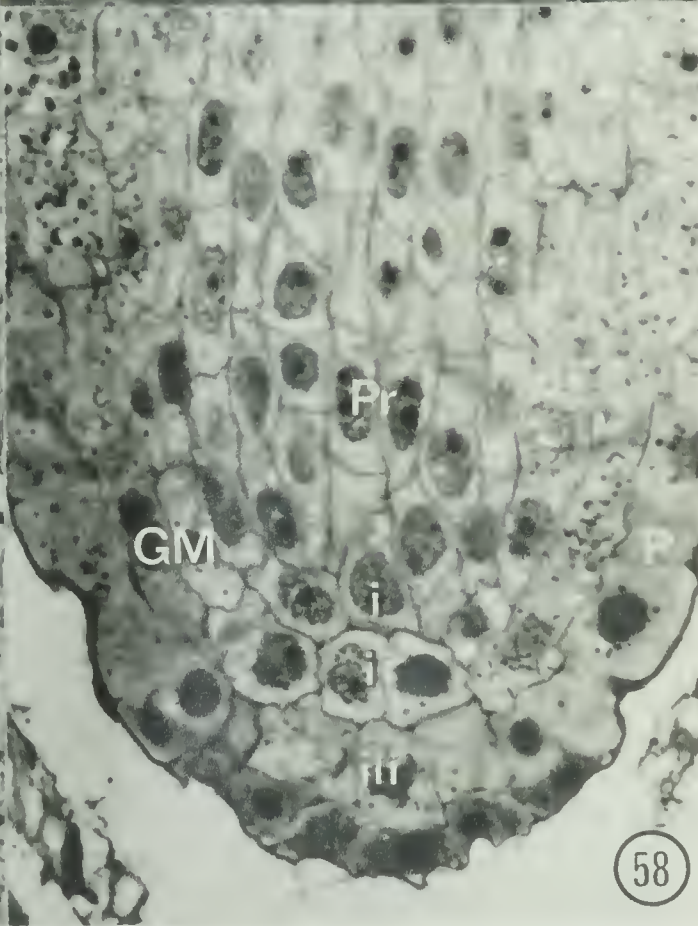
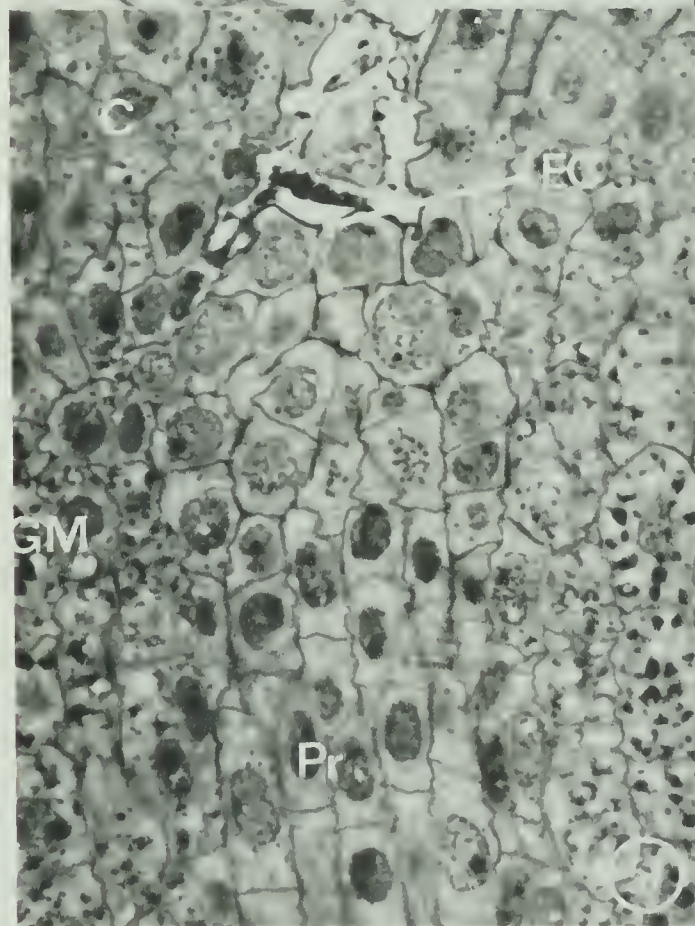
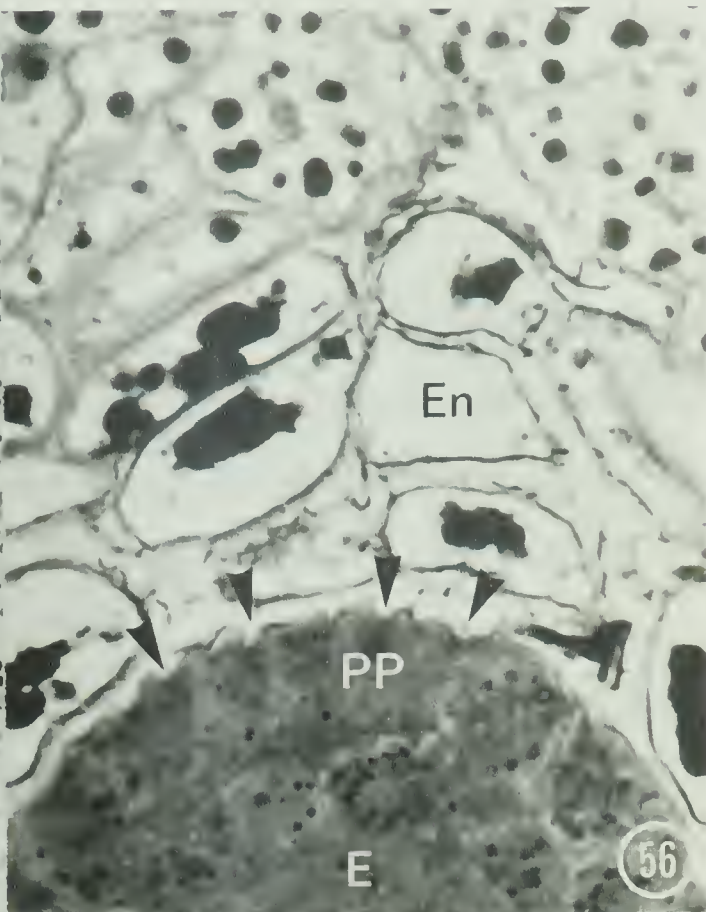
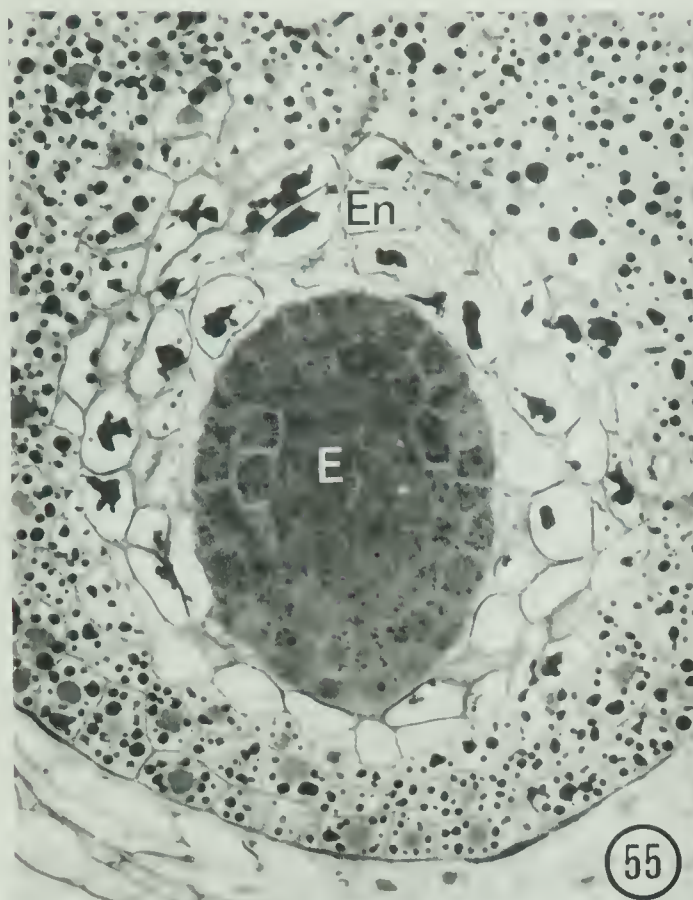
- Fig. 48: Light micrograph of longitudinal section through mature embryonic root apex. The section is stained with PAS-ABB. Histogen regions are clearly distinguishable. x 958.
- Fig. 49: Light micrograph of longitudinal section through mature seed coat. The section is stained with PAS-ABB. Fiber formation in outer epidermis of inner integument (3) is complete. Outer epidermis of outer integument (1) is the mechanical layer. x 1197.
- Fig. 50: Light micrograph of longitudinal section through entire mature albuminous seed produced in vitro. The section is stained with methylene blue. x 194.



- Fig. 51: Light micrograph of longitudinal section through two-celled pro-embryo 4 days after hand pollination in vivo. The section is stained with PAS-ABB. x 987.
- Fig. 52: Light micrograph of oblique section through antipodals 4 days after hand pollination in vivo. The section is stained with PAS-ABB. Arrows indicate well developed antipodal wall ingrowths. x 729.
- Fig. 53: Light micrograph of longitudinal section through micropylar end of seed 9-10 days after hand pollination in vivo. The section is stained with PAS-ABB. Note symmetrical pattern of endosperm degradation with embryo as the focus. x 400.
- Fig. 54: Light micrograph of longitudinal section through globular embryo 12 days after hand pollination in vivo. The section is stained with PAS-ABB. Suspensor cells stain less intensely than cells of embryo proper. x 707.



- Fig. 55: Light micrograph of longitudinal section through embryo 14-15 days after hand pollination in vivo. The section is stained with PAS-ABB. Incipient protoderm is crenulated. x 427.
- Fig. 56: Light micrograph of embryo-endosperm interface detail 14-15 days after hand pollination in vivo (same as in Fig. 55). The section is stained with PAS-ABB. Arrowheads indicate crenulations in outer tangential walls of incipient protoderm. Endosperm degradation greatest near the embryo. x 1176.
- Fig. 57: Light micrograph of longitudinal section through embryonic shoot apex region in mature seed produced in vivo. The section is stained with PAS-ABB. Note the randomly arranged cells of the epicotyl. x 680.
- Fig. 58: Light micrograph of longitudinal section through embryonic root apex region in mature seed produced in vivo. The section is stained with PAS-ABB. Histogen regions and their derivatives are discernable. x 680.



CHAPTER FOUR

SUMMARY AND CONCLUSIONS

Placental pollination and subsequent fertilization in vitro are relatively recent phenomena (Kanta et al., 1962). Early studies using the in vitro placental pollination technique were primarily concerned with achieving successful fertilization and seed set in a variety of angiosperms and whether or not the seeds produced in vitro were viable (Kanta and Maheshwari, 1963; Maheshwari and Kanta, 1964). The more recent studies attempted to improve the technique and increase the percentage of seed set (Balatková and Tupý, 1972; Balatková et al., 1977). The present study of Papaver nudicaule is the first attempt to document internal morphological aspects of seed development in vitro and compare the results to selected morphological stages of seed development in vivo. There are at least two major conclusions that can be drawn from the present study of P. nudicaule. First, in vitro placental pollination, fertilization, and seed development result in germinable seeds. Germination is defined as radicle emergence from the seed coat. A few of the seeds produced in vitro germinated while still attached to the placenta and some of these eventually established seedlings. In most cases, however, the seeds had to be detached from the placenta and sown on fresh medium before either germination and/or seedling establishment took place. The second conclusion is that internal morphological development in vitro generally compares well with development in vivo. The number of days required to reach a particular developmental stage and the degree

of embryo differentiation at the time of seed "maturation" are the major differences between the in vitro and in vivo systems. Possible interpretations of these differences are discussed in the previous chapter.

The systematic embryology of the Papaveraceae is incomplete (Davis, 1966). The more recent reports on Argemone mexicana (Sachar, 1955), Dendromecon rigida (Berg, 1967), and Eschscholzia californica (Sachar and Ram, 1958; Negi, 1974) surveyed and characterized different reproductive and structural aspects of the family. The present study is an attempt to relate major internal morphological events to one another during seed ontogeny in a member of the Papaveraceae. The major contribution of the present study, however, is the implied potential usefulness of the Papaver nudicaule placental pollination system as a research tool from the morphological and experimental data. Both pre- and post-fertilization ovules of P. nudicaule possess not only various internal structural components that may be of interest to angiosperm embryologists, but the developmental processes can be initiated and maintained in vitro which may broaden the spectrum of interest in such a system to include plant physiologists and biochemists as well.

The data from the present study suggest at least six major areas of ovule and seed biology that may be explored further by using both pre- and post-pollination placental cultures of P. nudicaule.

1. Ovule nutrition -- There is a structural relationship between the funicular strand, the hypostase, and the anti-podals. Fine structural examination accompanied by autoradiographic experimentation may demonstrate a physiological relationship between these ovule components as well.

2. Pollen tube-ovule interaction -- Erotropic guidance, if it exists, of pollen tubes into the ovules is not understood.

Pollinated placentae may be subjected to histochemical procedures in an attempt to localize possible ovular exudates.

3. Fertilization -- In P. nudicaule, in vitro fertilization occurs between 24 and 31 hours post-pollination. It should be possible to refine the timing of megagametophyte penetration, gamete transfer, and sperm fusion with egg and polar nuclei in order to examine these events with the electron microscope.

4. Embryo nutrition -- There appears to be an interdependent morphological relationship between embryo development and endosperm breakdown. The incipient protoderm may be directly involved in endosperm degradation and/or metabolite absorption. Crenulations first develop in the entire incipient protoderm of the globular embryo, but are eventually restricted in later embryogenesis to the tips of the cotyledons. Fine structural investigation might provide evidence to support the notion that the protoderm is the site of synthesis for endosperm degradation factors (Masand and Kapil, 1966). The morphological clarity of endosperm degradation makes P. nudicaule ideal for histochemical procedures designed to localize enzyme activity.

5. Environmental effects on seed ontogeny -- There is evidence to support the hypothesis that fertilization and seed ontogeny are physiologically adapted to their environmental

temperature (Balatkova et al., 1977). The Papaver in vitro system can be subjected to a variety of temperature regimes to determine the limits and optimum temperature for the developmental process. The effects of extreme temperature on seed development may also be elucidated. The number of variables that may influence the results of experiments where the developing seeds are still contained in the parental sporophyte is reduced.

6. Seed dormancy -- Papaver seeds produced in vitro are capable of germination shortly after achieving morphological maturity, but usually require detachment from the placenta. Does the placenta produce inhibitors or do toxic metabolic wastes from placental deterioration interfere with the germination process? In vitro manipulation of variables such as water potentials and hormone levels during seed development and germination may provide insight into the internal controls, if any, of hypocotyl elongation and radicle emergence.

The practical applications of placental pollination in vitro to the horticultural and agricultural industries were first cited by Kanta et al. (1962). The sexual union of gametes that would otherwise be prevented from fusion in nature is now possible. Horticulturalists, for example, interested in achieving self-fertilization and seed set in a particular ornamental species that is self-incompatible may be able to circumvent the problem in vitro. Gynoecial barriers to self-fertilization in Petunia have been successfully by-passed in the test-tube (Rangaswamy and Shivanna, 1967). Development of hybrid food crops between related taxa that are presently unsuccessful because

of various pollen-gynoecial incompatibilities may be possible in vitro. Intra-generic and inter-generic hybridizations have been achieved with in vitro placental pollination in the Caryophyllaceae (Zenkteler, 1967). Similar hybridization experiments have been attempted in members of different families with limited success, but because fertilization did occur, the results are encouraging (Zenkteler, 1970). Further experimentation and procedural refinement is necessary before widespread use of in vitro fertilization techniques of this nature is feasible on a commercial scale. The full economic impact of placental pollination, fertilization, and seed development in vitro has yet to be realized.

BIBLIOGRAPHY

- Alpi, A., F. Tognoni, and F. D'Amato. 1975. Growth regulator levels in embryo and suspensor of Phaseolus coccineus at two stages of development. *Planta* 127: 153-162.
- Ashley, T. 1972. Zygote shrinkage and subsequent development in some Hibiscus hybrids. *Planta* 108: 303-317.
- Balatková, V. and J. Tupý. 1968. Test-tube fertilization in Nicotiana tabacum by means of an artificial pollen tube culture. *Biol. Plantarum* 10: 266-270.
- _____. and _____. 1972. Some factors affecting the seed set after in vitro pollination of excised placentae of Nicotiana tabacum L. *Biol. Plantarum* 14: 82-88.
- Balatková, V., J. Tupý, and E. Hrabětová. 1977. Seed formation in Narcissus pseudonarcissus L. after placental pollination in vitro. *Plant Science Letters* 8: 17-21.
- Berg, R. Y. 1967. Megagametogenesis and seed development in Dendromecon rigida (Papaveraceae). *Phytomorphology* 17: 223-233.
- Bersillon, G. 1955. Recherches sur les Papaveracees. Contribution a l'etude du developpement des dicotyledones herbacees. *Annls. Sci. nat. Bot.* 16: 225-448.
- Bewley, J. D. and M. Black. 1978. *Physiology and Biochemistry of Seeds in Relation to Germination*. Springer-Verlag, New York.
- Brewbaker, J. L. and B. H. Kwack. 1963. The essential role of calcium ion in pollen germination and pollen tube growth. *Amer. J. Bot.* 50: 859-865.
- Brink, R. A. and D. C. Cooper. 1944. The antipodals in relation to abnormal endosperm behavior in Hordeum jubatum x Secale cereale hybrid seeds. *Genetics* 29: 391-406.
- Bronner, R. 1975. Simultaneous demonstration of lipids and starch in plant tissues. *Stain technol.* 50: 1-4.
- Buell, K. M. 1952a. Developmental morphology in Dianthus. I. Structure of the pistil and seed development. *Amer. J. Bot.* 39: 194-210.
- _____. 1952b. Developmental morphology in Dianthus. II. Starch accumulation in ovule and seed. *Amer. J. Bot.* 39: 458-467.

- Buvat, R. 1952. Structure, évolution et fonctionnement du méristème apical de quelques dicotylédones. *Annls. Sci. nat. Bot.* 13: 199-300.
- Cass, D. D. and W. A. Jensen. 1970. Fertilization in Barley. *Amer. J. Bot.* 57: 62-70.
- Cionini, P. G., A. Bennici, A. Alpi, and F. D'Amato. 1976. Suspensor gibberellin and in vitro development of Phaseolus coccineus embryos. *Planta* 131: 115-117.
- Coe, G. E. 1954. Distribution of carbon 14 in ovules of Zephyranthes drummondii. *Bot. Gaz.* 115: 342-346.
- Corcoran, M. R. and B. O. Phinney. 1962. Changes in amounts of gibberellin-like substances in developing seed of Echinocystis, Lupinus, and Phaseolus. *Physiol. Plantarum* 15: 252-262.
- Corner, E. J. H. 1976. The Seeds of Dicotyledons. Cambridge University Press, Cambridge.
- Coulter, J. M. and C. J. Chamberlain. 1912. Morphology of Angiosperms. D. Appleton and Co., New York.
- Crété, P. 1956. A propos de l'embryologie de l'Argemone mexicana. *Phytomorphology* 6: 144-148.
- _____. 1957. Embryogénie des Papavéracées. Le développement de l'embryon chez le Dicranostigma franchetianum. *C. R. Acad. Sci. Paris* 245: 720-722.
- Cutter, E. G. 1971. Plant Anatomy: Experiment and Interpretation. Part 2. Organs. Edward Arnold (Publishers) Ltd., London.
- Davies, H. V. and J. M. Chapman. 1979a. The control of food mobilisation in seeds of Cucumis sativus L. I. The influence of the embryonic axis and testa on protein and lipid degradation. *Planta* 146: 579-584.
- _____. and _____. 1979b. The control of food mobilisation in seeds of Cucumis sativus L. II. The role of the embryonic axis. *Planta* 146: 585-590.
- Davis, G. L. 1961. The occurrence of synergid haustoria in Cotula australis (Less) Hook. f. (Compositae). *Aust. J. Sci.* 24: 296.
- _____. 1962. Embryological studies in the Compositae. II. Sporogenesis, gametogenesis, and embryogeny in Ammobium alatum R. Br. *Aust. J. Bot.* 10: 65-75.
- _____. 1966. Systematic Embryology of the Angiosperms. J. Wiley and Sons, New York.

- Diboll, A. G. 1968. Fine structural development of the megagametophyte of Zea mays following fertilization. Amer. J. Bot. 55: 787-806.
- _____. and D. A. Larson. 1966. An electron microscopic study of the mature megagametophyte in Zea mays. Amer. J. Bot. 53: 391-402.
- Endress, A. G. and W. W. Thomson. 1976. Ultrastructural and cytochemical studies on the developing adhesive disc of Boston Ivy tendrils. Protoplasma 88: 315-331.
- Esau, K. 1977. Anatomy of Seed Plants. 2nd ed. J. Wiley and Sons, New York.
- Fahn, A. 1974. Plant Anatomy. 2nd ed. Pergamon Press, Oxford.
- Feder, N. and T. P. O'Brien. 1968. Plant microtechnique: some principles and new methods. Amer. J. Bot. 55: 123-142.
- Fisher, D. B. 1968. Protein staining of ribboned epon sections for light microscopy. Histochemie 16: 92-96.
- Foster, A. D. and E. M. Gifford. 1974. Comparative Morphology of Vascular Plants. 2nd ed. W. A. Freeman and Company, San Francisco.
- Glenk, H. O., W. Wagner, and O. Schimmer. 1971. Can Ca^{++} ions act as a chemotropic factor in Oenothera fertilization? In: Pollen Development and Physiology. J. Heslop-Harrison, ed. Butterworth, London.
- Gunning, B. E. S. and J. S. Pate. 1969. Transfer cells: Plant cells with wall ingrowths, specialized in relation to short distance transport of solutes -- their occurrence, structure, and development. Protoplasma 68: 107-133.
- Halmer, P., J. D. Bewley, and T. A. Thorpe. 1975. Enzyme to break down lettuce endosperm cell wall during gibberellin and light induced germination. Nature 258: 716-718.
- _____, _____, and _____. 1976. An enzyme to degrade lettuce endosperm cell walls. Appearance of a mannanase following phytochrome and gibberellin induced germination. Planta 130: 189-196.
- Hanstein, J. 1868. Die Scheitelzellgruppe im Vegetationspunkt der Phanerogamen. Festschr. Niederrhein. Gesell. Natur- und Heilkunde. 1868: 109-134.
- Herth, W., W. W. Franke, H. Bittiger, A. Kuppel, and G. Keilich. 1974. Alkali-resistant fibrils of B-1, 3- and B-1, 4- glucans: structural polysaccharides in the pollen tube wall of Lilium longiflorum. Cytobiologie 9: 344-367.
- Huss, H. A. 1906. Beiträge zur Morphologie und Physiologie der Antipoden. Beih. bot. Ztbl. 20: 77-174.

- Ikuma, H. and K. Thimann. 1963. The role of seed coats in germination of photosensitive lettuce seeds. *Plant and Cell Physiol.* 4: 169-185.
- Jensen, W. A. 1962. *Botanical Histochemistry*. W. A. Freeman and Company, San Francisco.
- _____. 1965a. The ultrastructure and histochemistry of the synergids of cotton. *Amer. J. Bot.* 52: 238-256.
- _____. 1965b. The ultrastructure and composition of the egg and central cell of cotton. *Amer. J. Bot.* 52: 781-797.
- _____. 1968. Cotton embryogenesis: The zygote. *Planta* 79: 346-366.
- _____. and D. B. Fisher. 1968. Cotton embryogenesis: The entrance and discharge of the pollen tube in the embryo sac. *Planta* 78: 158-183.
- Johansen, D. A. 1940. *Plant Microtechnique*. McGraw-Hill, Inc., New York.
- Jones, R. L. 1974. The structure of the lettuce endosperm. *Planta* 121: 133-146.
- Kanta, K., N. S. Rangaswamy, and P. Maheshwari. 1962. Test-tube fertilization in a flowering plant. *Nature* 194: 1214-1217.
- _____. and P. Maheshwari. 1963. Test-tube fertilization in some angiosperms. *Phytomorphology* 13: 230-237.
- Kaplan, D. R. 1969. Seed development in Downingia. *Phytomorphology* 19: 253-278.
- List, A. and F. C. Steward. 1965. The nucellus, embryo sac, endosperm, and embryo of Aesculus and their interdependence during growth. *Ann. Bot. N. S.* 29: 1-15.
- Lorenzi, R., A. Bennici, A. Alpi, and F. D'Amato. 1976. Suspensor gibberellin and in vitro development of Phaseolus coccineus embryos. *Planta* 131: 115-117.
- Luckwill, L. C. 1948. The hormone content of the seed in relation to endosperm development and fruit drop in the apple. *Jour. Hort. Sci.* 24: 32-44.
- _____. 1953. Studies of fruit development in relation to plant hormones. I. Hormone production by the developing apple seed in relation to fruit drop. *Jour. Hort. Sci.* 28: 14-24.
- Machlis, L. 1972. The coming of age of sex hormones in plants. *Mycologia* 64: 235-247.
- Maheshwari, N. 1958. In vitro culture of excised ovules of Papaver somniferum. *Science* 127: 342.

- Maheshwari, N. and M. Lal. 1961. In vitro culture of excised ovules of Papaver somniferum L. Phytomorphology 11: 307-314.
- Maheshwari, P. 1948. The angiosperm embryo sac. Bot. Rev. 14: 1-56.
- _____. 1950. An Introduction to the Embryology of Angiosperms. McGraw-Hill, New York.
- _____. and K. Kanta. 1964. Control of fertilization. In: Pollen Physiology and Fertilization. H. F. Linskens (ed.) North-Holland, Amsterdam.
- Marinos, N. G. 1970. Embryogenesis of the pea (Pisum sativum). I. The cytological environment of the developing embryo. Protoplasma 70: 261-279.
- Masand, P. and R. N. Kapil. 1966. Nutrition of the embryo sac and embryo -- A morphological approach. Phytomorphology 16: 158-175.
- Mascarenhas, J. P. 1966. The distribution of ionic calcium in the tissues of the gynoecium of Antirrhinum majus. Protoplasma 62: 53-58.
- _____. and L. Machlis. 1962. Chemotropic responses of Antirrhinum majus pollen to calcium. Nature 196: 292-293.
- Matile, Ph. 1976. Vacuoles. In: Plant Biochemistry. 3rd ed. James Bonner and Joseph Varner (eds). Academic Press, New York.
- Meunier, A. 1891. Les téguments sémiaux des Papavéracées. Cellule 7: 375-412.
- Miller, H. A. and R. H. Wetmore. 1945. Studies in the developmental anatomy of Phlox drummondii Hook. I. The embryo. Amer. J. Bot. 32: 588-599.
- Mogensen, H. L. 1972. Fine structure and composition of the egg apparatus before and after fertilization in Quercus gambelii: The functional ovule. Amer. J. Bot. 59: 931-941.
- _____. 1978. Pollen tube-synergid interactions in Proboscidea louisianica (Martineaceae). Amer. J. Bot. 65: 953-964.
- Morrison, I. N. and T. P. O'Brien. 1976. Cytokinesis in the developing wheat grain; division with and without a phragmoplast. Planta 130: 57-67.
- Mukherjee, R. K., A. Bhanja, and S. M. Sircar. 1966. Growth substances separated from the fruits of Cassia fistula. Physiol. Plantarum 19: 448-458.

- Negi, D. S. 1974. Ultrastructure of the Female Gametophyte of Eschscholzia californica Before and After Fertilization. Ph.D. dissertation. University of California, Berkeley.
- Newcomb, W. 1973a. The development of the embryo sac of sunflower Helianthus annuus before fertilization. Can. J. Bot. 51: 863-878.
- _____. 1973b. The development of the embryo sac of sunflower Helianthus annuus after fertilization. Can. J. Bot. 51: 879-890.
- _____. 1978. The development of cells in the coenocytic endosperm of the African blood lily Haemanthus Katherinae. Can. J. Bot. 56: 483-501.
- _____. and L. C. Fowke. 1973. The fine structure of the change from the free nuclear to cellular condition in the endosperm of chickweed Stellaria media. Bot. Gaz. 134: 236-241.
- _____. and _____. 1974. Stellaria media embryogenesis: the development and ultrastructure of the suspensor. Can. J. Bot. 52: 607-614.
- _____. and T. A. Steeves. 1971. Helianthus annuus embryogenesis: embryo sac wall projections before and after fertilization. Bot. Gaz. 132: 367-371.
- Nitsch, J. P. 1951. Growth and development in vitro of excised ovaries. Amer. J. Bot. 38: 566-577.
- Ogawa, Y. 1963a. Changes in the content of gibberellin-like substances in ripening seed and pod of Lupinus luteus. Plant Cell Physiol. 4: 85-94.
- _____. 1963b. Gibberellin-like substances occurring in the seed of Pharbitis nil Choisy and their change in contents during seed development. Plant Cell Physiol. 4: 217-225.
- Pate, J. S. and B. E. S. Gunning. 1972. Transfer cells. Ann. Rev. Plant Physiol. 23: 173-196.
- Pontovich, V. É. and I. N. Sveshnikova. 1966. Formation of Papaver somniferum L. embryos in ovules cultured in vitro. Fiziol. Rastenii. 13: 91-102. (English translation).
- Popham, R. A. 1966. Laboratory Manual for Plant Anatomy. C. V. Mosby Company, St. Louis.
- Pritchard, H. N. 1964. A cytochemical study of embryo sac development in Stellaria media. Amer. J. Bot. 51: 371-378.
- Raghavan, V. 1976. Experimental Embryogenesis in Vascular Plants. Academic Press, London.

- Ramsey, J. C. and J. D. Berlin. 1976. Ultrastructure of early stages of cotton fiber differentiation. *Bot. Gaz.* 137: 11-19.
- Rangaswamy, N. S. and K. R. Shivanna. 1967. Induction of gamete compatibility and seed formation in axenic cultures of a diploid self-incompatible species of Petunia. *Nature* 216: 937-939.
- Reeve, R. M. 1948. The "tunica-carpus" concept and development of shoot apices in certain dicotyledons. *Amer. J. Bot.* 35: 65-75.
- Röder, I. 1958. Anatomische und fluoreszenzoptische Untersuchungen an Samen von Papaveraceen. *Ost. bot. Z.* 104: 370-381.
- Sachar, R. C. 1955. The embryology of Argemone mexicana L. -- A reinvestigation. *Phytomorphology* 5: 200-218.
- _____. 1956. The embryology of Argemone mexicana L. -- A criticism. *Phytomorphology* 6: 148-151.
- _____. and H. Y. M. Ram. 1958. The embryology of Eschscholzia californica. *Phytomorphology* 8: 114-124.
- _____. and M. Kapoor. 1959. In vitro culture of ovules of Zephyranthes. *Phytomorphology* 9: 147-156.
- Sass, J. E. 1958. Botanical Microtechnique. 3rd ed. The Iowa State University Press, Ames.
- Schmidt, A. 1924. Histologische Studien an phanerogamen Vegetationspunkten. *Bot. Arch.* 8: 345-404.
- Schulz, S. R. and W. A. Jensen, 1968a. Capsella embryogenesis: the synergids before and after fertilization. *Amer. J. Bot.* 55: 541-552.
- _____. and _____. 1968b. Capsella embryogenesis: the egg, zygote, and young embryo. *Amer. J. Bot.* 55: 807-819.
- _____. and _____. 1969. Capsella embryogenesis: the suspensor and basal cell. *Protoplasma* 67: 139-163.
- _____. and _____. 1973. Capsella embryogenesis: the central cell. *J. Cell Sci.* 12: 741-763.
- Schürhoff, P. N. 1926. Die Zytologie der Blütenpflanzen. Ferdinand Enke Verlag, Stuttgart.
- Sedgley, M. 1979. Light microscope study of pollen tube growth, fertilization and early embryo and endosperm development in the Avocado varieties Fuerte and Hass. *Ann. Bot.* 44: 353-359.

- Shaw, C. H. 1904. Note on the sexual generation and the development of seed-coats in certain of the Papaveraceae. Bull. Torrey Bot. Club 31: 429-433.
- Shivanna, K. R. 1965. In vitro fertilization and seed formation in Petunia violacea Lindl. Phytomorphology 15: 183-185.
- Souéges, R. 1926. Embryogénie des Papavéracées. Développement du proembryon chez le Papaver Rhoeas L. C. R. Acad. Sci., Paris 183: 902-904.
- _____. 1928. Développement de l'embryon chez le Papaver Rhoeas L. Bull. Soc. bot. France 75: 452-469.
- _____. 1948. Embryogénie des Papavéracées. Développement de l'embryon chez le Roemeria violacea (R. hybrida). C. R. Acad. Sci. Paris 226: 979-981.
- _____. 1949a. Embryogénie des Papavéracées. Développement de l'embryon chez l'Eschscholzia californica Cham. C. R. Acad. Sci. Paris 229: 485-487.
- _____. 1949b. Embryogénie des Papavéracées. Développement de l'embryon chez l'Argemone mexicana. C. R. Acad. Sci. Paris 229: 573-576.
- Spurr, A. R. 1969. A low-viscosity epoxy resin embedding medium for electron microscopy. J. Ultrastruct. Res. 26: 31-43.
- Stanley, R. G. 1971. Pollen chemistry and tube growth. In: Pollen Development and Physiology. J. Heslop-Harrison, ed. Butterworth, London.
- _____. and H. F. Linskens. 1974. Pollen: Biology, Biochemistry, and Management. Springer-Verlag, New York.
- Steeves, T. A. and I. M. Sussex. 1972. Patterns in Plant Development. Prentice-Hall, Inc. Englewood Cliffs, New Jersey.
- Stokes, P. 1952. A physiological study of embryo development in Heracleum sphondylium L. I. The effect of temperature on embryo development. Ann. Bot. N. S. 16: 441-447.
- Suzuki, T. 1963. A rapid staining method for light microscopy of plastic embedded sections. J. Electronmicroscopy (Japan) 12: 73-74.
- Sze, H. and F. M. Ashton. 1971. Dipeptidase development in cotyledons of Cucurbita maxima during germination. Phytochemistry 10: 2935-2942.
- Trump, B. F., E. A. Smuckler, and E. P. Benditt. 1961. A method for staining epoxy sections for light microscopy. J. Ultrastruct. Res. 5: 343-348.

- Usha, S. V. 1965. In vitro pollination in Antirrhinum majus L. Curr. Sci. 34: 1511-1513.
- Van der Pluijm, J. E. 1964. An electron microscopic investigation of the filiform apparatus in the embryo sac of Torenia fournieri. In: Pollen Physiology and Fertilization. H. F. Linskens (ed.) North-Holland, Amsterdam.
- Van Went, J. L. 1970a. The ultrastructure of the synergids of Petunia. Acta Bot. Neerl. 19: 121-132.
- _____. 1970b. The ultrastructure of the egg and central cell of Petunia. Acta Bot. Neerl. 19: 313-322.
- _____. 1970c. The ultrastructure of the fertilized embryo sac of Petunia. Acta Bot. Neerl. 19: 468-480.
- Villiers, T. A. and P. F. Wareing. 1964. Dormancy in fruits of Fraxinus excelsior L. J. Exp. Bot. 15: 359-367.
- Wareing, P. F. and I. D. J. Philips. 1978. The Control of Growth and Differentiation in Plants. 2nd ed. Pergamon Press, Inc., New York.
- Werker, E., I. Marbach, and A. M. Mayer. 1979. Relation between the anatomy of the testa, water permeability, and the presence of phenolics in the genus Pisum. Ann. Bot. 43: 765-771.
- Yeung, E. C. and M. E. Clutter. 1979. Embryogeny of Phaseolus coccineus: the ultrastructure and development of the suspensor. Can. J. Bot. 57: 120-136.
- Zenkteler, M. 1967. Test-tube fertilization of ovules in Melandrium album Mill. with pollen grains of several species of the Caryophyllaceae family. Experimentia 23: 775-776.
- _____. 1970. Test-tube fertilization of ovules in Melandrium album Mill. with pollen grains of Datura stramonium L. Experimentia 26: 661-662.

APPENDIX ONE

Tissue treatment schedule for plastic embedding.

TREATMENT	TIME (HRS.)	TEMP. (C)
3% glutaraldehyde in phosphate buffer (pH 6.8)	3	5
PO ₄ buffer (pH 6.8)	.75	5
PO ₄ buffer (pH 6.8)	.75	5
2% osmium tetroxide in phosphate buffer (pH 6.8)	2	5
PO ₄ buffer (pH 6.8)	.5	5
PO ₄ buffer (pH 6.8)	.5	5
20% ethanol	.5	5
30% ethanol	.5	5
40% ethanol	.5	5
50% ethanol	.5	5
60% ethanol	.5	5
70% ethanol	.5	5
80% ethanol	.5	5
90% ethanol	.5	5
100% ethanol	10	5
100% ethanol	1	20
1:1 100% ethanol to propylene oxide	1	20
propylene oxide	1	20
propylene oxide	1	20
propylene oxide	1	20

TREATMENT	TIME (HRS.)	TEMP. (C)
20% resin	24	20
40% resin	24	20
60% resin	24	20
80% resin	24	20
100% resin	8	20
Polymerize in Beem capsules	24	60-70

Staining procedures for plastic embedded ovules.

Methylene blue (Suzuki, 1963)

Thick sections were:

1. Stained with 1% methylene blue in 50% ethanol with 1 ml of 5% KOH added to the solution at 60C.
2. Washed with H_2O .
3. Dried at 60C.
4. Mounted in Clearmount.

Toluidine blue (adapted from Trump et al., 1961)

Thick sections were:

1. Stained with 1% aq. toluidine blue in 1% aq. borax at 60C for 10 minutes.
2. Washed with dH_2O .
3. Dried at 60C.
4. Mounted in Clearmount.

Aniline Blue Black (Fisher, 1968)

Thick sections were:

1. Stained in 1% aniline blue black in 7% acetic acid at 50-60C for 10 minutes.
2. Washed in 7% acetic acid.
3. Dried at 60C.
4. Mounted in Clearmount.

Period acid-Schiff's Reaction (Feder and O'Brien, 1968)

Thick sections were:

1. Treated with 0.5% periodic acid for 30 minutes.
2. Rinsed in running H₂O for 1 hour.
3. Treated with Schiff's reagent for 1 hour.
4. Rinsed in running H₂O for 1 hour.
5. Dried at 60C.
6. Mounted in water (for counter staining) or Clearmount.

Sudan black B (Bronner, 1975)

Semithin sections (0.5um) were:

1. Treated with 70% ethanol for 1-2 minutes.
2. Treated with 0.3% Sudan black B in 70% ethanol for 1 hour in an oven (60C).
3. Rinsed in 70% ethanol for 1 minute.
4. Rinsed in H₂O.
5. Mounted in glycerin.

Aniline blue fluorescence (adapted from Jensen, 1962)

Both thick sections and whole ovules were:

1. Treated with 0.005% aniline blue in 0.15M phosphate buffer (pH 9.5) for 0.5 hours.

2. Mounted in the aniline blue staining solution.

3. Observed using UV fluorescence on Zeiss Photomicroscope II.

Excitation filters I and IV (300-500nm) and barrier filter 47 or 53.

APPENDIX TWO

In vitro technique and culture medium.

1. One day before anthesis, flower buds were opened, emasculated, and bagged to prevent pollination.
2. The unpollinated gynoecia were collected 48-72 hours after anthesis. Whole anthers that were just beginning to dehisce were collected and placed under UV light for 30 minutes.
3. Gynoecia were surface sterilized (alcohol-flaming) and the intact placentae were dissected out in a transfer room. Free placentae were immediately transferred to a pollination plate. (The pollination plate is a sterile petri dish with a thin layer of growth medium in one of the halves.)
4. Pollen was scooped out of the anthers into a sterile petri dish with a sterile dissecting needle.
5. Pollen was collected on a sterile cotton ball and dusted over the placentae in the pollination plate.
6. Two to three pollinated placentae were transferred to each culture tube and incubated at 23C.

A surgical mask was worn during all dissections and tissue transfers. All tissues were handled with alcohol-flamed instruments.

Modified Nitsch's growth medium:

(See: Nitsch, 1951; Maheshwari and Lal, 1961)

$\text{Ca}(\text{NO}_3)_2 \times 4\text{H}_2\text{O}$	500 mg/L
KNO_3	125 mg/L
$\text{MgSO}_4 \times 7\text{H}_2\text{O}$	125 mg/L
KH_2PO_4	125 mg/L
glycine	7.5 mg
niacin	1.2 mg
thiamine	0.25 mg
pyridoxine	0.25 mg
calcium pantothenate	0.25 mg
agar	8.0 g
sucrose	50.0 g
Solution A (ferric citrate)	1 cc
Solution B (trace element mixture)	1 cc

1. Add dH_2O to the above to make 1 full liter. Slowly heat until all components go into solution.
2. Adjust pH to 5.8.
3. Pour 5-8 ml of the solution into each culture tube, cap, and autoclave at 15 lbs for 15 minutes.

To make Solution A (ferric citrate solution):

1. Add dH_2O to 10 g of $\text{FeC}_6\text{O}_5\text{H}_7 \times 5\text{H}_2\text{O}$ to make up 1 liter of solution.
2. Autoclave separately at 15 lbs for 15 minutes.

To make Solution B (trace element mixture):

1. Make a 1 liter solution containing trace elements

H_2SO_4 (sp. gr. 1.83)	0.5 cc/L
$\text{MnSO}_4 \times 4\text{H}_2\text{O}$	3000 mg/L
$\text{ZnSO}_4 \times 7\text{H}_2\text{O}$	500 mg/L
H_3BO_4	500 mg/L
$\text{CuSO}_4 \times 5\text{H}_2\text{O}$	25 mg/L
$\text{Na}_2\text{MoO}_4 \times 2\text{H}_2\text{O}$	25 mg/L

2. Autoclave separately at 15 lbs for 15 minutes.

B30295